FINAL REPORT

Novel Atmospheric High Power Impulse Plasma Source for Durable, Field Applicable Coatings

SERDP Project WP-2608

APRIL 2020

Vasiliki Poenitzsch
Southwest Research Institute

Distribution Statement A
This document has been cleared for public release

SERDP
DOD ▪ EPA ▪ DOE

This report was prepared under contract to the Department of Defense Strategic Environmental Research and Development Program (SERDP). The publication of this report does not indicate endorsement by the Department of Defense, nor should the contents be construed as reflecting the official policy or position of the Department of Defense. Reference herein to any specific commercial product, process, or service by trade name, trademark, manufacturer, or otherwise, does not necessarily constitute or imply its endorsement, recommendation, or favoring by the Department of Defense.

REPORT DOCUMENTATION PAGE

Form Approved
OMB No. 0704-0188

Public reporting burden for this collection of information is estimated to average 1 hour per response, including the time for reviewing instructions, searching existing data sources, gathering and maintaining the data needed, and completing and reviewing this collection of information. Send comments regarding this burden estimate or any other aspect of this collection of information, including suggestions for reducing this burden to Department of Defense, Washington Headquarters Services, Directorate for Information Operations and Reports (0704-0188), 1215 Jefferson Davis Highway, Suite 1204, Arlington, VA 22202-4302. Respondents should be aware that notwithstanding any other provision of law, no person shall be subject to any penalty for failing to comply with a collection of information if it does not display a currently valid OMB control number. **PLEASE DO NOT RETURN YOUR FORM TO THE ABOVE ADDRESS.**

1. REPORT DATE *(DD-MM-YYYY)*
30-04-2020

2. REPORT TYPE
SERDP Final Report

3. DATES COVERED *(From - To)*
From 30 Sept 2016 To 29 Aug 2019

4. TITLE AND SUBTITLE
Novel Atmospheric High Power Impulse Plasma Source for Durable, Field Applicable Coatings

5a. CONTRACT NUMBER
W912HQ-16-C-0049

5b. GRANT NUMBER

5c. PROGRAM ELEMENT NUMBER

6. AUTHOR(S)
Vasiliki Z. Poenitzsch

5d. PROJECT NUMBER
WP-2608

5e. TASK NUMBER

5f. WORK UNIT NUMBER

7. PERFORMING ORGANIZATION NAME(S) AND ADDRESS(ES)
Southwest Research Institute
P.O. Drawer 28510
San Antonio, TX 78228-0510

8. PERFORMING ORGANIZATION REPORT NUMBER
22435.01

9. SPONSORING / MONITORING AGENCY NAME(S) AND ADDRESS(ES)
Strategic Environmental Research and Development Program
4800 Mark Center Drive, Suite 17D08
Alexandria, VA 22350-3600

10. SPONSOR/MONITOR'S ACRONYM(S)
SERDP

11. SPONSOR/MONITOR'S REPORT NUMBER(S)
WP-2608

12. DISTRIBUTION / AVAILABILITY STATEMENT
DISTRIBUTION STATEMENT A. Approved for public release: distribution unlimited.

13. SUPPLEMENTARY NOTES

14. ABSTRACT

The main objective of this effort was to investigate a novel atmospheric pressure, non-thermal High Power Impulse Plasma Source (HiPIPS) for deposition of field applicable coatings that meet military systems' technical requirements while reducing DoD's current systems' environmental and logistical footprints. The specific aims for this project were to i) investigate atmospheric pressure HiPIPS for deposition of durable protective coatings and ii) characterize the structural, mechanical and corrosion performance of the resultant coatings. SwRI has developed a promising atmospheric HiPIPS technique that provides an unparalleled plasma processing space of very high density, high flux plasmas at low temperature and atmospheric pressure conditions. The HiPIPS plasma jets, driven by advanced high power pulsed DC generators, produce extremely high power densities that can be used for the deposition of films. SwRI has conducted a systematic experimental study on the HiPIPS process parameters and resultant coating properties towards development of HiPIPS deposition of CoCr, Ti-6Al-4V and TiN coatings. Plasma properties were characterized using current-voltage probes and optical emission spectroscopy (OES). The microstructure and elemental composition of resulting deposited were examined using scanning electron microscopy (SEM) and energy-dispersive X-ray (EDX) spectroscopy. The crystallographic properties of the coatings were examined with X-ray diffraction (XRD). Pressure hardened 4340 steel and 7075 aluminum alloy substrate materials were evaluated. Control samples were prepared using chrome plating services by the Corpus Christi Army Depot. The corrosion and mechanical performance of these HiPIPS coatings were evaluated and compared with traditional chrome plated and uncoated alloys using GM 14872 accelerated corrosion test environment and fatigue testing per ASTM E466, respectively.

15. SUBJECT TERMS
Plasma, atmospheric pressure, non-thermal, coatings, deposition

16. SECURITY CLASSIFICATION OF:			17. LIMITATION OF ABSTRACT	18. NUMBER OF PAGES	19a. NAME OF RESPONSIBLE PERSON
a. REPORT	b. ABSTRACT	c. THIS PAGE			Vasiliki Z. Poenitzsch
U	U	U	UU	46	19b. TELEPHONE NUMBER *(include area code)* 210-522-3755

Standard Form 298 (Rev. 8-98)
Prescribed by ANSI Std. Z39.18

Table of Contents

Table of Contents vii
List of Tables ix
List of Figures xi
List of Acronyms xiii
Keywords xv
Abstract xvii
Executive Summary xix
1.0 Objectives 1
2.0 Background 1
2.1 SERDP Relevance 1
2.2 Background 1
3.0 Materials and Methods 3
3.1 Technical Approach 3
3.1.1 Task 1. Atmospheric High Power Impulse Plasma Source (HiPIPS) 4
3.1.2 Task 2. Characterization of Resultant Coatings 7
3.1.3 Task 3. Mechanical Testing and Evaluation 8
3.1.4 Task 4. Corrosion Testing and Evaluation 9
4.0 Results and Discussion 9
4.1 Results Summary 9
4.1.1 HiPIPS Plasma Process Space Investigations 9
4.1.2 HiPIPS Deposition Experiments 13
4.1.3 Control Sample Preparation 18
4.1.4 Corrosion Testing and Evaluation 19
4.1.5 Mechanical Testing and Evaluation 20
5.0 Conclusions and Implications for Future Research 22
5.1 Conclusions 22
5.2 Implications for Future Research 24
6.0 Literature Cited 25
Appendix A: List of Scientific/Technical Publications 27
Appendix B: Other Supporting Materials 29

List of Tables

Table 1. HiPIPS Process Parameters.....6
Table 2. Summary of stress-life test results. 21

List of Figures

Figure 1. (a) Photograph of HiPIPS Ar plasma demonstrating atmospheric, low temperature capability and (b) oscilloscope traces of voltage, current, and power during operation of HiPIPS.....3

Figure 2. Overall Program Plan. 4

Figure 3. Schematic of an atmospheric HiPIPS design for deposition of metallic films.....5

Figure 4. Photographs of (a)the original prototype HiPIPS jet head and (b) an improved HiPIPS jet head developed and manufactured in the program. 5

Figure 5. Photographs of HiPIPS set-up with customized X-Y substrate rastering stage. 7

Figure 6. Schematic and photograph of S-N dogbone specimens for mechanical testing.....9

Figure 7. Oscilloscope traces of voltage, current and power during the operation of the HiPIPS with Ar and (a) Ti-6Al-4V electrode and nozzle and (b) CoCr electrode and nozzle. 10

Figure 8. Optical emission spectrum and photograph (inset) during the operation of the HiPIPS with Ar and Ti electrode and nozzle. 11

Figure 9. Optical emission spectrum and photograph (inset) during the operation of the HiPIPS with Ar and Ti-6Al-4V alloy electrode and nozzle. 11

Figure 10. Optical emission spectrum and photograph (inset) during the operation of the HiPIPS with Ar and CoCr alloy electrode and nozzle. 12

Figure 11. Optical emission spectrum and photograph (inset) during the operation of the HiPIPS with Ar and N_2 and Ti electrode and nozzle. 13

Figure 12. Photographs depicting the evolution of preliminary HiPIPS deposition studies from static to dynamic on Si wafer substrates. Both exemplars shown are Ti-6Al-4V depositions. 13

Figure 13. SEM images of resultant deposits from two HiPIPS Ti-6Al-4V deposition experiments that depict how variation of HiPIPS process conditions can modify the result from synthesis of spherical nanoparticles towards deposition of a coating. 14

Figure 14. Cross-section SEM image of a HiPIPS CoCr coating on Si wafer. 14

Figure 15. Cross-section SEM micrograph (left) and corresponding EDS elemental maps of HiPIPS CoCr coating on 4340 steel substrate. EDS mapping analysis reveals coating layer contains uniform distribution and high amounts of cobalt and chromium. 15

Figure 16. Cross-section SEM micrograph (left) and corresponding EDS elemental maps of HiPIPS Ti-6Al-4V coating on 4340 steel substrate. The coating remains adhered after machining and polishing. EDS mapping analysis reveals that the coating layer contains uniform distribution and high amounts of titanium, vanadium and aluminum. 15

Figure 17. Photographs of as deposited coating from deposition processes using the HiPIPS with pure Ti electrode and (a) Ar gas only and (b) Ar and N_2 gas at 1:1 ratio. 16

Figure 18. EDS data of the deposited coating (shown in Figure 17a) from operation of HiPIPS with pure Ti electrode and Ar. 17

Figure 19. EDS data of the deposited coating (shown in Figure 17b) from operation of HiPIPS with pure Ti electrode and 1:1 of $Ar:N_2$. 17

Figure 20. XRD of the as-deposited HiPIPS coating using Ti electrode and 1:1 ratio of $Ar:N_2$. 18

Figure 21. Photograph of exemplary Cr-plated 4340 steel dogbone tensile specimens and 4340 steel corrosion test panels obtained from CCAD. 18

Figure 22. Photographs of samples after 15 cycles of GMW 14872 testing on 4340 steel substrates. The coatings tested included the SwRI-developed HiPIPS coatings as well as coatings applied using conventional plating techniques and uncoated samples for comparison. 19

Figure 23. Photographs of samples after 42 cycles of GMW 14872 testing on 7075 aluminum alloy substrates. The coatings tested included the SwRI-developed HiPIPS coatings as well as coatings applied using conventional plating techniques and uncoated samples for comparison. 19

Figure 24. Photograph of HiPIPS Ti6Al4V deposition process on dog-bone fatigue sample specimen. The HiPIPS plasma head remained stationary as the dog-bone specimen was translated and rotated during the deposition process. 20

Figure 25. Comparison of fatigue lives at 155 ksi for the four conditions evaluated (baseline and three surface treatments). 22

List of Acronyms

Acronym	Definition
AFM	Atomic Force Microscope
AMCOM	United States Army Aviation and Missile Command
AP	Atmospheric Pressure
ASTM	American Society for Testing and Materials
CCAD	Corpus Christi Army Depot
CRA	Corrosion Resistant Alloy
DARPA	Defense Advanced Research Projects Agency
DC	Direct Current
DoD	Department of Defense
EDS	Energy Dispersive Spectroscopy
EHC	Electrolytic Hard Chrome Plating
EPA	Environmental Protection Agency
HiPIPS	High Power Impulse Plasma Source
HVOF	High Velocity Oxygen Fuel
PEL	Permissible Exposure Limit
PI	Principle Investigator
NAVAIR	Naval Air Systems Command
OEM	Original Equipment Manufacturer
OES	Optical Emission Spectroscopy
OSHA	Occupational Safety and Health Administration
SEM	Scanning Electron Microscope
SERDP	Strategic Environmental Research and Development Program
SOA	State of Art
SwRI	Southwest Research Institute
TRL	Technical Readiness Level
US	United States
VOC	Volatile Organic Compound

Keywords

Plasma, atmospheric pressure, coatings, deposition

Abstract

Introduction and Objectives: Atmospheric pressure, non-thermal plasma deposition for durable protective coatings is a promising candidate to replace electroplating and revolutionize coating technologies that address Department of Defense (DoD) life-cycle cost and environmental issues related to weapons systems. The objectives of this project were to investigate a novel atmospheric pressure, non-thermal High Power Impulse Plasma Source (HiPIPS) for deposition of field applicable, protective coatings and characterize the structural, mechanical, and corrosion performance of the resultant coatings.

Technical Approach: SwRI conducted a systematic experimental study on the HiPIPS process parameters and resultant coating properties towards development of HiPIPS deposition of CoCr, Ti6Al4V, and TiN coatings. Using HiPIPS, Ar-initiated metallic Ti, CoCr, or Ti-6Al-4V plasmas were generated and the plasma properties were characterized by measuring current-voltage characteristics and optical emission spectroscopy (OES). Pressure hardened 4340 steel and 7075 aluminum alloy substrate materials were evaluated. The corrosion (cyclic accelerated corrosion test, GM 14872) and mechanical performance (fatigue testing per ASTM E466) of the HiPIPS coatings were evaluated and compared with traditional chrome plated and uncoated alloys. The chrome plating was performed by the Corpus Christi Army Depot (CCAD). The microstructure and chemical composition of the resulting HiPIPS coatings were examined using scanning electron microscopy (SEM), energy-dispersive X-ray (EDX) spectroscopy, X-ray diffraction, and nanoindentation.

Results: Altogether, the results of this project advanced the atmospheric pressure HiPIPS technique to TRL 4, validation in a laboratory environment to apply durable, metallic coatings. HiPIPS investigations with Ar and N_2 gas and Ti, CoCr, or Ti-6Al-4V wires confirmed our hypothesis that high peak power pulses can be achieved (10-70 kW) resulting in high peak currents (100-250 A) and increased ionization and plasma density while maintaining low overall power (40W) and substrate processing temperatures (< 50 °C). OES spectral measurements confirm the presence of metal ions with high photon intensities in HiPIPS plasmas. HiPIPS CoCr, Ti-6Al-4V and TiN coatings were successfully deposited. Cross-section SEM analysis and EDS mapping revealed uniform coatings. The nano-hardness of HiPIPS TiN, Ti6Al4V and CoCr films ranged from 11.56 to 14.09, 3.92 to 4.44, and 6.20 to 8.42 GPa, respectively. In GM 14872 accelerated corrosion test environment, the HiPIPS applied Ti6Al4V and CoCr coatings showed slightly more corrosion damage than the conventional coatings, but significantly less than that of the uncoated sample. Under fatigue testing per ASTM E466, the HiPIPS Ti6Al4V coatings had a similar stress-life response as baseline, uncoated performance and the HiPIPS CoCr coatings were approximately half the fatigue life of the baseline conditions.

Benefits: The project provided vital insight needed for the development of a new deposition technology that could reduce the costs and environmental risks in maintenance and replacement of military components. The HiPIPS process is attractive for the repair or replacement of electroplated hard chromium in line-of-sight applications. HiPIPS is non-thermal, atmospheric pressure plasma capable of producing highly ionized species for deposition of durable metallic films. Additionally, HiPIPS could allow for coating removal, pre-cleaning, and coating using the same equipment and varying process parameters. A HiPIPS system is portable and can be operated in versatile environments. Further development work is required to further increase the technology readiness level and identify specific applications.

Executive Summary

Introduction

Materials degradation due to wear, fatigue, and corrosion impedes combat readiness and costs multiple billions of dollars in the maintenance and replacement of components. Currently, electroplating processes, such as hard chromium and nickel plating, are used to protect the surfaces of wear and fatigue sensitive parts and to rebuild damaged components. Electrolytic hard chrome plating (EHC) is one of the most widely used surface treatment processes throughout the military services. EHC is used by original equipment manufacturers (OEMS) for applying hard, wear-resistant coating and by repair depots for general re-build of worn or corroded components. Yet, hard chrome plating utilizes chromium in the hexavalent state (hex-Cr), a known carcinogen, and represents a significant contribution to hazardous, carcinogens waste generation and pollution control costs. The U.S. Occupational Safety and Health Administration (OSHA) regulates worker hexavalent chromium permissible exposure limits (PEL) to 5 µg/m3. Transportation and regulatory costs for repairing metallic plated components are significant expenses for traditional military weapon system life-cycles. Increasingly stringent U.S. OSHA and Environmental Protection Agency (EPA) regulations will continue to drive up costs in the use of hex-Cr processes. There is an expanding need for the ability to execute metallic coating repair operations on low-risk military items and components to minimize transportation and regulatory costs and maintain combat readiness levels. Yet, existing state-of-the-art (SOA) metallic coating repair processes have operational, regulatory, and infrastructure footprints that limit ability for front line maintenance applications. Beyond environmental and health concerns, are also concerns with in-service performance of chrome plating with decreasing Department of Defense (DoD) maintenance budgets and increasing life cycle of military systems. Thus, cost-effective, deployable coating alternatives are critical to achieving both the military environmental goals and the performance of key components throughout the services.

Existing technologies being explored as alternatives to chrome electroplating include High Velocity Oxygen Fuel (HVOF), thermal and cold spray techniques. While these technologies have shown promise for deposition of hard coatings, they have limitations for field use. To enable field repair and integrate smoothly with existing maintenance and repair procedures, an ideal replacement technique would not require extensive pre- or post-coating processing. HVOF and cold spray technologies, while promising technologies in many ways, often require extensive machining after deposition to recover the intended dimensions. This limits the ability of the coating techniques to be field-deployable and complicates the repair. HVOF processes have large logistical footprints and high operational costs limiting use as deployable units for field repair. Cold spray processes are more deployable but they also rely on powdered feed material. This requirement has limited the material selection for application, in several cases complicating its application and approval.

Metallic or ceramic coatings are commonly deposited using a vacuum process such as a physical vapor deposition (PVD) or a plasma assisted chemical vapor process (PACVD). PVD of Cr, CrN, Ti and TiN is an industrially mature technology utilized to deposit hard coatings with high resistance to wear, corrosion and heat. Yet, a vacuum chamber is needed so that plasma can be generated fairly easily at a low gas pressure typically from a few millitorr to a few hundred torr. Although the coating quality of vacuum-based process is quite high, the process has to be performed inside a vacuum system is very cumbersome and expensive. For some applications,

vacuum deposition is impossible as in field repair coating and/or coating of larger structures. An atmospheric pressure (AP) plasma deposition process would be very attractive and practical.

To overcome the vacuum chamber and high temperature processing, SwRI is developing a novel atmospheric pressure, non-thermal High Power Impulse Plasma Source (HiPIPS) technique for deposition of coatings. HiPIPS operates very differently from thermal plasma spray processes. The HiPIPS technology is an advanced variation of atmospheric pressure plasma process that allows for enhanced ~~sur~~face~~-~~ modi~~f~~ication ~~a~~nd dep~~o~~sition of functional coatings. The HiPIPS technology, consisting of an advanced pulsed DC generator in combination with atmospheric pressure plasma jets, provides an unparalleled plasma processing space of very high density and flux at low temperature and atmospheric pressure conditions. Preliminary results indicate that HiPIPS plasmas outperforms SOA ambient pressure non-thermal plasmas in areas such as power, current, precursor dissociation and flux, ion energy and precursor diversity, and rivals SOA vacuum plasma systems in many of these same categories. In this project, a variation of HiPIPS that employs a solid metal wire source material is developed and investigated.

Objectives

The main objective of this effort was to investigate a novel atmospheric pressure, non-thermal HiPIPS for deposition of field applicable and durable protective coatings that meet military systems' technical requirements while reducing DoD's current systems' environmental and logistical footprints. The specific aims for this proposed program were to i) investigate atmospheric pressure HiPIPS for deposition of durable protective coatings and ii) characterize the structural, mechanical and corrosion performance of the resultant coatings.

Technical Approach

HiPIPS Process: SwRI conducted a systematic experimental study on the HiPIPS process parameters and resultant coating properties towards development of HiPIPS deposition of CoCr, Ti6Al4V, and TiN coatings. Using HiPIPS, Ar-initiated metallic Ti, CoCr, or Ti-6Al-4V plasmas were generated. A design for HiPIPS is schematically shown in Figure E-1. The HiPIPS jet head fundamentally consists of a metal wire feed stock (the electrode), a metal tube, a ceramic tube and a metal nozzle. Metal wires were nominally 0.32 cm in diameter and metal tubes were nominally 1.2 cm in diameter and 4 cm in length. The metal wire was centered axially in the tube and the tip was positioned within ≤ 2 mm from the end of the nozzle. Driven by a pulsed DC power supply (Liaoning Beiyu Vacuum Science and Technology Co), the HiPIPS jet head was used at atmospheric pressure for various processes including plasma cleaning and deposition of metallic or ceramic coatings. The HiPIPS plasmas were operated in ambient room conditions without a controlled environment chamber. When the working gas is fed and DC pulses at certain peak voltage, frequency and pulse width are applied to the center electrode of the HiPIPS, plasma is generated between the electrode and the metal nozzle, resulting in the ablation of the electrode and the nozzle materials. As the DC pulse continues the current increases dramatically. Due to the high current capability of the advanced power supply design, extremely high peak power can be applied into the plasma within a short period of time. This high power discharge leads to the production of highly ionized gases. The advanced micropulsing capability of the power generator restricts discharge times to values below the time constant for instabilities.

A number of depositions were carried out to study the effect of deposition parameters, such as pulse power and frequency, precursor gas, and deposition pressure, on the formation of thin films. We employed HiPIPS to generate metallic plasmas at atmospheric pressure using different source metal wires consisting of CrCo alloy, Ti-6Al-4V alloy, and Ti wires (0.125 in diameter). The operating range for HiPIPS during deposition was as follows. High purity Ar (99.995%) was used as the working gas and the flow rate controlled by a mass flow controller (MKS Instruments Model 247D) was varied from 3 to 20 slm. The pulsed voltage was varied from 0.6 to 2.5 kV, while the pulse frequency was fixed at 500 Hz with the pulse width fixed at 20 µs.

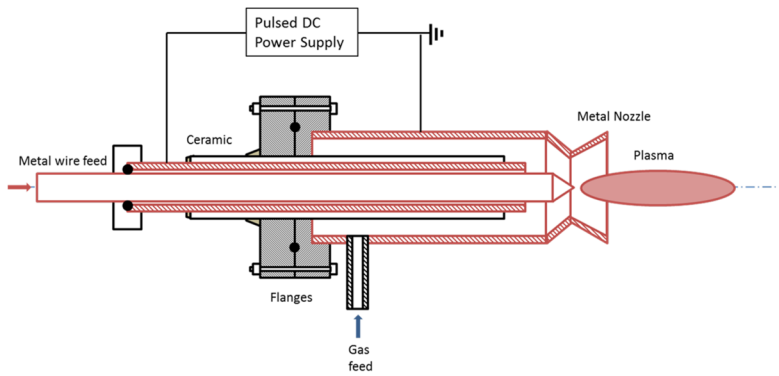

Figure E-1. *A schematic diagram of HiPIPS system. Line filled areas represent air gaps.*

The distance between the plasma source and the substrate surface was set to approximately 8 mm. Standard silicon wafers (25 x 25 x 0.75 mm), 4340 steel coupons and 7075 aluminum coupons (8 x 13 x 0.64 cm) were used as substrates. Depositions were conducted using a customized X-Y substrate rastering stage. The films were deposited in multiple passes ranging from 3 to 10 passes at a scan velocity of 10 mm/s and a step size of 1 mm. A negative bias ranging from 70 to 120 V was applied to the substrates during deposition. The 4340 steel substrates were mechanically polished to remove existing roughness and surface oxides. All substrates were solvent cleaned with isopropyl alcohol and air dried before deposition. Bonding layer treatments evaluated including applying negative bias to the substrate and atmospheric pressure plasma processing using compressed air or hexamethyldisiloxane (HMDSO) gas precursors.

Plasma Characterization: Optical emission spectroscopy (OES), electrical probes and a Langmuir probe were employed for measuring and calculating the plasma characteristics and their variation with systematic changes in HiPIPS process parameters and conditions. An Ocean Optics HR4000CG-UV-NIR spectrometer fitted with a 3648-element linear-array charge-coupled device (CCD) detector provided high resolution ($\Delta\lambda$ = 0.75 nm) emission spectra throughout a 200 to 1000 nm wavelength range. All spectra were acquired through optical fiber at distance of 10 cm between the fiber aperture and the plasma source. Absolute intensity calibrations were performed using two radiance calibration standards traceable to NIST. OES spectroscopic data were acquired without automatic noise subtraction and are shown herein without any numerical processing. The electrical properties of the HiPIPS plasma were studied by measuring the voltage and current transients across the discharge. The measurements were made using a high voltage probe (Tektronix P6015A) and an inductive current monitor (Pearsons Electronics Model 4418). The results were recorded on a digital oscilloscope (Tektronix).

Control Sample Preparation: Corpus Christi Army Depot (CCAD) provided chrome plating

services, performed to CCAD Process Specification B-OO, to fabricate control samples for comparison testing in the project.

Coating Characterization: Scanning electron microscopy (JEOL 5800LV SEM) was used for microstructural examination of the resultant coatings. Energy-dispersive X-ray (EDS) spectroscopy along with EDS mapping was used to determine film elemental composition. Cross-sectional analysis was conducted on coated 4340 samples that were cut, mounted and polished. The crystallographic properties of coatings were investigated with an X-ray diffractometer (XRD, Siemens KRISTALLOFLEX 805). The nanohardness of HiPIPS thin films were obtained by nanoindentation technique (Hysitron Triboscope, USA). Load controlled indentation testing followed a trapezoidal loading profile with a hold time of typically 10 s at peak load. Peak loads were ranged from 3000 to 5000 μN. The diamond indenter was a Berkovich tip with a tip radius of 100 nm. X-ray Diffraction (XRD) analysis was carried out on the surface of the as-deposited samples using a Siemens KRISTALLOFLEX 805 XRD in a Bragg-Brentano configuration (Cu

Kα radiation generated at 40 kV and 25 mA).

Mechanical Testing: Constant-amplitude load-controlled fatigue testing was performed per ASTM E466 on baseline, Cr plated and HiPIPS coated 4340 steel alloys in order to assess the effect on the fatigue performance. A dog-bone based fatigue geometry was selected that integrated into test fixtures already available at SwRI's Solid and Fracture Mechanics Laboratory. The gage section of the coupon was longitudinally polished to achieve a consistent surface finish and minimal residual stress as is critical in fatigue life testing. A servohydraulic test frame was utilized to apply the constant amplitude loading of the coupons. A stress ratio (ratio of minimum load to maximum load) of 0.1 was used during testing with a cyclic rate of 10 Hz. Testing was performed in laboratory ambient conditions, namely 72 °F and 30-50%. Using baseline coupons, a maximum cyclic stress of 155 ksi was chosen for this focused investigation. The resulting fatigue life at this cyclic stress condition was near 100,000 cycles. A total of three baseline coupons were tested while a minimum of five coupons were tested for each coating.

Corrosion Testing: The corrosion performance of the HiPIPS coatings were evaluated and compared with traditional chrome plated and uncoated 4340 steel and 7075 aluminum alloys using GM 14872 accelerated corrosion test. A total of three coupons were tested for baseline and each coating.

Results and Discussion

HiPIPS utilizes atmospheric pressure plasma jets with high power pulsed DC generators that supply extremely high power densities in short pulses of tens of microseconds at low duty cycles. The development of HiPIPS plasma source involved experiments where the process parameters were systematically varied to examine their effects on the resulting HiPIPS plasma. HiPIPS investigations with argon gas and Ti, CoCr, and Ti-6Al-4V wires confirmed that high peak power pulses can be achieved (10 - 70 kW), resulting in high peak currents (100 - 250 A) and increased ionization and plasma density while maintaining low average power (40W) and substrate processing temperatures (<50 °C) (Figure E-2). Figure E-2b shows a snap shot of the voltage, current and power traces for one pulse of HiPIPS running with Ar gas and Ti-6Al-4V electrode. The typical high peak currents (166 A) and high peak powers (76 kW) in the pulse can be observed. Other parameters such as the peak voltage of 2.46 kV, pulse frequency of 500 Hz and pulse width of 20 μs can be seen on the oscilloscope readouts.

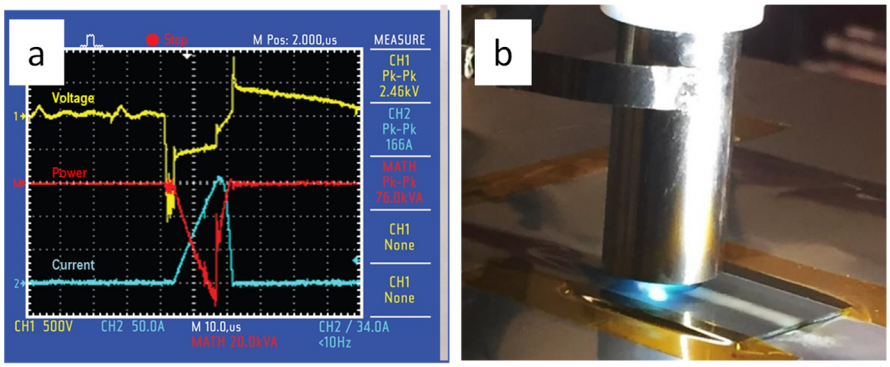

Figure E-2. *(a) Voltage, current and power traces for one pulse of HiPIPS running with Ar gas and Ti-6Al-4V electrode. (b) Photograph of HiPIPS Ti6Al4V deposition on a 1 in x 1 in substrate.*

Optical emission spectroscopy (OES) provided quantitative plasma diagnostics through measurement of optical emissions from excited states of species, usually formed by electron impact excitation of respective ground state species. Figure E-3 shows the optical emission spectra measured for HiPIPS plasma with a Ti6Al4V wire interacting with Ar gas. The vertical axes of the figures indicate the number of photons or intensity. All spectra are shown as measured without noise subtraction or numerical processing. A number of atomic lines are clearly observed. The lines observed in the 690 - 820 nm range are characteristic of Ar in both wavelength and relative intensities. The lines observed in the 320 - 670 nm range are assigned to Ti I and Ti II. Moreover, the high relative intensity and common transition probability for Ti I line at wavelength $\lambda = 521$ nm and the Ti II line at wavelength $\lambda = 670$ nm are present. Additional lines are present for Al and V, such as the Al I line at $\lambda = 400$ nm and the V I line at $\lambda = 420$ nm. From the inset photograph, one can clearly see the bright plasma characteristics of HiPIPS.

The metallic emission line intensities results from a two-step process. First, metallic atoms (Ti, Co, Cr, Al) are sputtered from the wire by Ar ions:

$$Ar^{+} + \text{Metal Wire} \Rightarrow M^{+*} \qquad (1)$$

Second, these sputtered species are excited either by secondary electrons to form metal excited states:

$$M^{+} + e^{-1} \Rightarrow M^{*} \qquad (2)$$

Likewise, OES spectra for HiPIPS operated with Ar and CoCr wire electrode exhibited spectral lines for Ar, Co, and Cr. Lines in the 690 - 820 nm range are again characteristic of Ar. The strongest emission line at $\lambda = 525$ nm is for Cr I. Other numerous Cr I and Cr II lines are present between 220and 550 nm. Also present are atomic lines for Co I in the 320-375 nm region and at $\lambda = 575$ and 612 nm.[17] Altogether, the OES spectra have successfully detected and identified charged states of the excited species in the plasma that will ultimately form the deposited coatings.

HiPIPS Ti-6Al-4V and CoCr alloy coating deposition process conditions on 4340 steel substrates were developed through a series of trials where a pulsed voltage range of 0.6-2.5 kV with the pulse frequency fixed at 500Hz and the pulse width fixed at 20 µs, a flow rate of 15 slm of Ar, and a substrate bias range of 70 to 100 V were utilized. To get to a uniform coating surface coverage it required at least 8 passes or coating layers. Shown in Figure E-4 is a cross-section SEM micrograph

and corresponding EDS elemental maps representative of HiPIPS CoCr coating. As can be observed in the SEM image, the coating remains adhered after machining and polishing the 4340 steel substrate. Typical coating thickness varied from 1 to 5 µm depending on deposition time. The average deposition rate was approximately 64 nm/sec. EDS mapping analysis reveals that the coating layer contains high amounts and uniform distributions of chromium and cobalt. The elemental composition of the resultant coating can be correlated to the excited species observed in the OES spectra of the HiPIPS CoCr plasma. Likewise, shown in Figure E-5 is a cross-section SEM micrograph and corresponding EDS elemental maps of HiPIPS Ti-6Al-4V coating. The Ti-6Al-4V coating also remains adhered after machining and polishing the 4340 steel substrate. The EDS elemental maps reveal that the coating layer contains uniform distribution and high amounts of Ti, Al, and V. The elemental composition of the resultant coating can be correlated to the excited species observed in the OES spectra of the HiPIPS Ti-6Al-4V plasma.

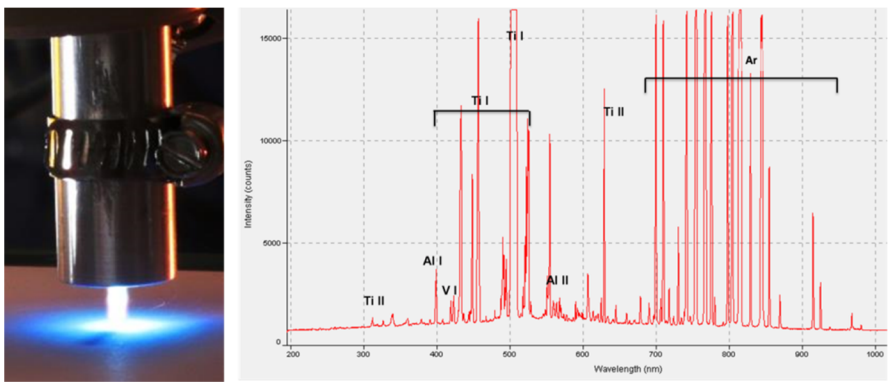

Figure E-3. *Photograph (left) and OES spectrum (right) during the operation of HiPIPS with Ar and Ti-6Al-4V wire electrode. OES spectral measurements confirm the presence of* Ti^* *and* Ti^{+*} *along with* Al^**,* Al^{+*} *and* V^* *with high photon intensities in the HiPIPS plasma.*

Deposition trials towards a TiN coating were conducted using HiPIPS with pure Ti electrode and nozzle and addition of nitrogen gas to argon gas. Using pure nitrogen gas would result in only N_2 plasma and no coating deposition without energetic Ar ions to sputter the wire electrode. We systematically varied the ratio of Ar and N_2 and settled on a ratio of 1:1 for deposition trials. The inset of Figure E-6 shows photograph of as deposited coatings on Si wafers from deposition process using the HiPIPS with pure Ti electrode with Ar and N_2 gas at 1:1 ratio. The coating has the characteristic goldish color of TiN coating. EDS data of the HiPIPS deposition on Si wafer using Ti electrode with Ar and N_2 confirmed that nitrogen is indeed observed in the elemental composition of the film. A representative XRD spectrum of the as-deposited HiPIPS film on stainless steel substrate using Ti electrode with Ar and N_2 gas at 1:1 ratio is shown in Figure E-6. The diffraction peaks related to (111) and (200) crystalline planes of titanium nitride are observed. Titanium nitride diffraction peaks are in agreement with the Joint Committee for Powder Diffraction Standards. The nanohardness of HiPIPS thin films were obtained by nanoindentation technique where the peak loads ranged from 3000 to 5000 µN. The nanohardness measured for HiPIPS Ti6Al4V and CoCr films ranged from 3.92 to 4.44 and 6.20 to 8.42 GPa, respectively.

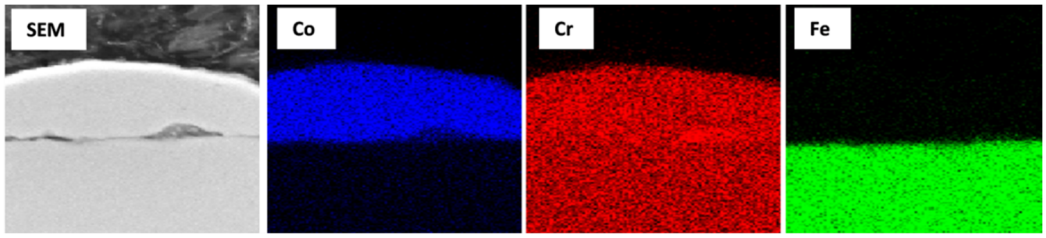

Figure E-4. *Cross-section SEM micrograph (left) and corresponding EDS elemental maps of HiPIPS CoCr coating on 4340 steel substrate. The coating remains adhered after machining. EDS mapping analysis reveals coating layer contains uniform distribution and high amounts of cobalt and chromium.*

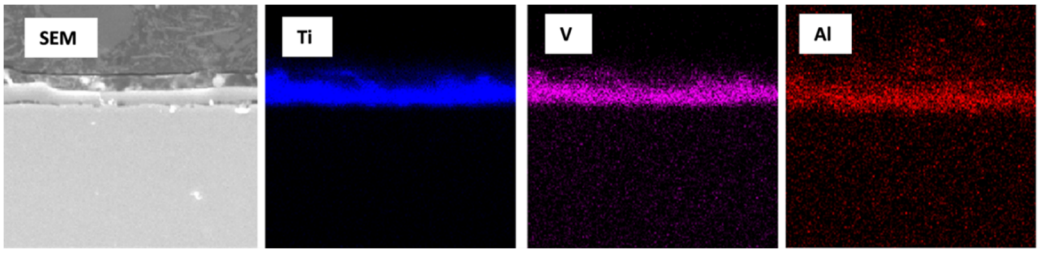

Figure E-5. *Cross-section SEM micrograph (left) and corresponding EDS elemental maps of HiPIPS Ti-6Al-4V coating on 4340 steel substrate. The coating remains adhered after machining. EDS mapping analysis reveals coating layer contains uniform distribution and high amounts of titanium, aluminum, and vanadium.*

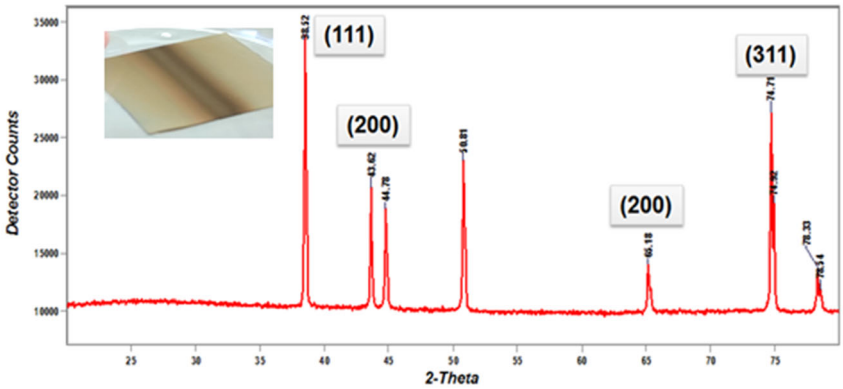

Figure E-6. *XRD of and (inset) photograph of as-deposited HiPIPS coating using Ti electrode and 1:1 ratio of Ar:N_2.*

SwRI completed GMW 14872 testing on coated and uncoated 4340 steel samples. The coatings tested include the SwRI-developed atmospheric plasma coatings as well as coatings applied using conventional plating techniques and uncoated samples for comparison. All steel coupons exhibited significant amounts of corrosion after 15 cycles of testing, including the conventionally plated samples. The atmospheric plasma-applied Ti6Al4V and CoCr coatings on steel substrates showed more corrosion damage than the conventional coatings, but significantly less than that of the uncoated sample (Figure E-7). All steel coupons were removed from the chamber after 15 cycles of testing. SwRI also completed GMW 14872 testing on SwRI-developed HiPIPS CoCr coatings, SwRI HiPIPS SiOx bond layer coating, conventional Cr plating techniques (CCAD plating), and uncoated samples 7075 aluminum alloy samples for comparison. Aluminum coupons were tested

for 42 cycles, longer than the 15 cycles for the steel coupons because the coatings on the aluminum coupons were less affected by the cyclic test. The HiPIPS Ti6Al4V coating and the uncoated samples showed significant damage at the completion of this testing. The HiPIPS CoCr coating and HiPIPS organosiloxane base layer alone (< 200 nm) coatings performed better than the samples plated with the conventional coatings and the uncoated samples.

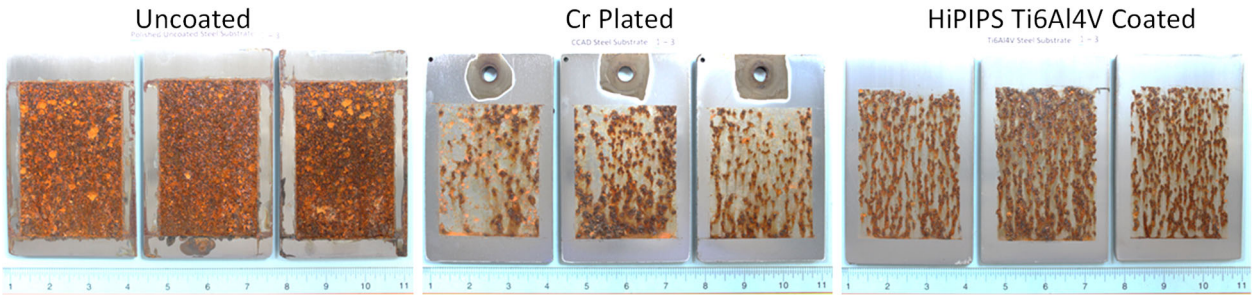

Figure E-7. *Photographs of samples after 15 cycles of GMW 14872 testing on 4340 steel substrates.*

While the application of surface coatings or treatments can enhance wear or corrosion resistance, it can also influence the fatigue performance, and as such it is important to characterize how the material responds under cyclic loading. Baseline fatigue performance was compared to three surface treatments that included: CCAD Cr plated, SwRI HiPIPS Ti6Al4V and SwRI HiPIPS CoCr. Comparison of fatigue performance was based on a maximum stress level of 155 ksi which provided finite fatigue lives for all conditions. A bar-chart is presented in Figure E-8 for the test results at 155 ksi max stress for all conditions evaluated. When comparing the three surface treatments, there appears to be three distinct groups of fatigue lives. The HiPIPS Ti6Al4V had the highest fatigue life followed by the HiPIPS CoCr and the CCAD condition demonstrating the lowest fatigue life. When comparing the baseline response, the HiPIPS Ti6Al4V had a similar stress-life response. The CCAD Cr Plated, on the other hand, was approximately an order of magnitude shorter in life. The SwRI HiPIPS CoCr was approximately half the fatigue life of the baseline conditions. When visually evaluating the fracture surfaces of the failed coupon, surface crack initiation followed by crack growth was the mode of failure. It is important to note that the CCAD condition demonstrated numerous surface cracks along the gage length with one of those cracks becoming the dominant crack and cause of failure. Recall the CCAD condition had an order of magnitude reduction in life compared to the baseline. This high population of surface cracks supports the significant reduction in life.

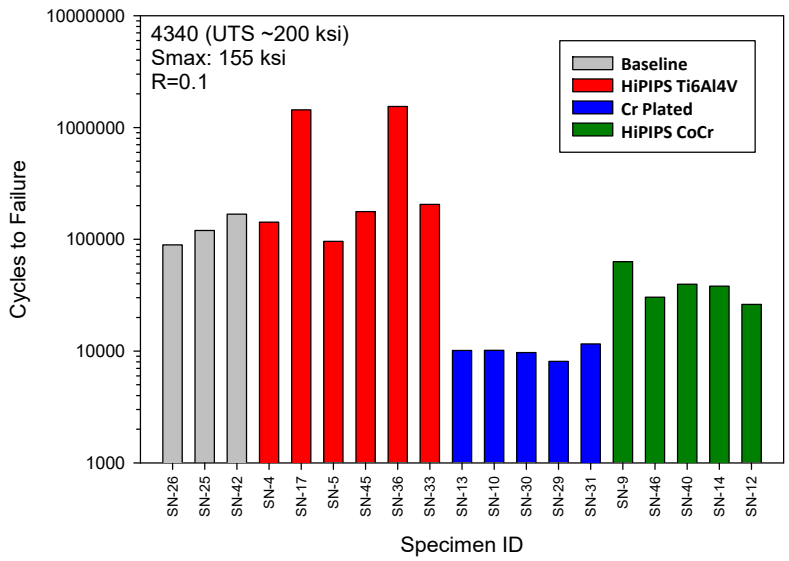

Figure E-8. *Comparison of fatigue lives at 155 ksi for the four conditions evaluated (baseline, Cr Plated and two HiPIPS coatings).*

Implications for Future Research and Benefits

Altogether, the results of the project met the main objective to investigate a novel atmospheric pressure, non-thermal HiPIPS for deposition of durable protective coatings and characterize the structural, mechanical and corrosion performance of the resultant coatings. The project provided vital insight needed for the development of a new deposition technology that could reduce the costs and environmental risks in maintenance and replacement of military components. The results of this project advanced the atmospheric pressure HiPIPS technique to TRL 4, validation in a laboratory environment to apply durable, metallic coatings. HiPIPS technology is unique in that this technology generates high density, high flux plasmas at low temperature and atmospheric pressure conditions. The HiPIPS technology provides an unparalleled plasma space that extends conventional atmospheric pressure plasma (APP) applications and allows for deposition of metallic coatings at ambient conditions. HiPIPS eliminates the need for vacuum chambers, high temperature processing and in-spray scenarios in surface treatments and deposition of coatings.

The HiPIPS process is attractive for the repair or replacement of electroplated hard chromium in line-of-sight applications. HiPIPS is non-thermal, atmospheric pressure plasma capable of producing highly ionized species for deposition of durable films. Processing temperatures are $\leq$ 150 °C. HiPIPS operates solely with an inert carrier gas (i.e., Ar, N_2) and solid metallic wire/rod source material. While this project focused on demonstration of CoCr, Ti6Al4V, and TiN films, the HiPIPS process is widely applicable to other coating chemistries. Additionally, HiPIPS could allow for coating removal, pre-cleaning, and coating using the same equipment and varying process parameters. Substrates require no special surface preparation, substrate heating, or extensive post-treatments. HiPIPS has a fine level of control over deposition thickness, reducing post application machining. A HiPIPS system is portable and can be operated in versatile environments. Further development work is required to increase the technology readiness level and identify specific applications.

1.0 Objectives

The main objective of this effort was to investigate a novel atmospheric pressure, non-thermal HiPIPS for deposition of field applicable and durable protective coatings that meet military systems' technical requirements while reducing DoD's current systems' environmental and logistical footprints. The specific aims for this proposed program were to i) investigate atmospheric pressure HiPIPS for deposition of durable protective coatings and ii) characterize the structural, mechanical and corrosion performance of the resultant coatings.

Current state-of-art (SOA) non-thermal atmospheric pressure plasma technologies do not have capability to deposit durable, protective metallic coatings. Under funding from DARPA, SwRI developed an innovative HiPIPS technology that generates high density pulsed plasmas using advanced pulsed DC generators in combination with atmospheric pressure plasma jets. The technique was at a Technical Readiness Level (TRL) of 2, meaning that the concept is formulated and a proof-of-concept to a specific application was required to increase the TRL of atmospheric HiPIPS. The goal of this work was to advance the atmospheric HiPIPS technique to TRL 4: validation in a laboratory environment to apply durable protective coatings that reduce or eliminate dependence on electro-deposition technologies.

2.0 Background

2.1 SERDP Relevance

Electrolytic hard chrome plating (EHC) is one of the most widely used surface treatment processes throughout the military services. EHC is used by original equipment manufacturers (OEMS) for applying hard, wear-resistant coating and by repair depots for general re-build of worn or corroded components [1-2]. Yet, hard chrome plating utilizes chromium in the hexavalent state (hex-Cr), a known carcinogen, and represents a significant contribution to hazardous, carcinogens waste generation and pollution control costs. The U.S. Occupational Safety and Health Administration (OSHA) regulates worker hexavalent chromium permissible exposure limits (PEL) to 5 μg/m3. Transportation and regulatory costs for repairing metallic plated components are significant expenses for traditional military weapon system life-cycles. Increasingly stringent U.S. OSHA and Environmental Protection Agency (EPA) regulations will continue to drive up costs in the use of hex-Cr processes. There is an expanding need for the ability to execute metallic coating repair operations on low-risk military items and components to minimize transportation and regulatory costs and maintain combat readiness levels. Beyond environmental and health concerns, are also concerns with in-service performance of chrome plating with decreasing Department of Defense (DoD) maintenance budgets and increasing life cycle of military systems. Thus, cost-effective, deployable coating alternatives are critical to achieving both the military environmental goals and the performance of key components throughout the services.

2.2 Background

Materials degradation due to wear, fatigue, and corrosion impedes combat readiness and costs multiple billions of dollars in the maintenance and replacement of components [1-2.]. Currently, electroplating processes, such as hard chromium and nickel plating, are used to protect the surfaces of wear and fatigue sensitive parts and to rebuild damaged components. However, it is well known

that hexavalent chromium (Cr^{+6}) is a carcinogen that causes several environmental and health problems. Nickel is subject to increasingly strict environmental and health requirements, significantly complicating its use and disposal. To limit the use of these toxic chemicals, the materials and processes used to deposit the traditional coatings are being phased out both in the United States and around the world [1-2.]. Therefore, replacements which provide equivalent or improved performance without safety or environmental hazards are needed. These replacement coatings must have excellent wear and hardness properties. Additionally the replacement techniques must not result in any degradation of material processes such as overheating or embrittlement. Moreover, there is an expanding need for the ability to execute metallic coating repair operations on low-risk military items and components to minimize transportation and regulatory costs and maintain combat readiness levels. Yet, existing state-of-the-art (SOA) metallic coating repair processes have operational, regulatory, and infrastructure footprints that limit ability for front line maintenance applications.

Existing technologies being explored as alternatives to chrome electroplating include High Velocity Oxygen Fuel (HVOF), thermal and cold spray techniques [1-4]. While these technologies have shown promise for deposition of hard coatings, they have limitations for field use. To enable field repair and integrate smoothly with existing maintenance and repair procedures, an ideal replacement technique would not require extensive pre- or post-coating processing. HVOF and cold spray technologies, while promising technologies in many ways, often require extensive machining after deposition to recover the intended dimensions. This limits the ability of the coating techniques to be field-deployable and complicates the repair. HVOF processes have large logistical footprints and high operational costs limiting use as deployable units for field repair. Cold spray processes are more deployable but they also rely on powdered feed material. This requirement has limited the material selection for application, in several cases complicating its application and approval.

Metallic or ceramic coatings are commonly deposited using a vacuum process such as a physical vapor deposition (PVD) or a plasma assisted chemical vapor process (PACVD). PVD of Cr, CrN, Ti and TiN is an industrially mature technology utilized to deposit hard coatings with high resistance to wear, corrosion and heat [3]. Yet, a vacuum chamber is needed so that plasma can be generated fairly easily at a low gas pressure typically from a few millitorr to a few hundred torr. Although the coating quality of vacuum-based process is quite high, the process has to be performed inside a vacuum system is very cumbersome and expensive. For some applications, vacuum deposition is impossible as in field repair coating and/or coating of larger structures. An atmospheric pressure (AP) plasma deposition process would be very attractive and practical.

One existing method to deposit a coating using plasma at atmospheric pressure is to use a plasma spray system. Plasma spray is operated in the high power DC mode to achieve a flame temperature (12,000 - 20,000 °F) so that the metallic powder can be melt and hence deposited. The power requirement is typically in the range of a few hundred kW. To minimize the local overheating of the part, samples need to be rotated or move away quickly from the plasma torch. Due to the high power DC operation mode, the resultant coating is quite thick (typically in the range of 0.1 - 5 mm) and generally porous [4]. Thermal spray including HVOF, even though it does not utilize plasma, is still a high temperature process. Thermal processes are known to adversely affect components with degradation, embrittlement and fatigue life debit.

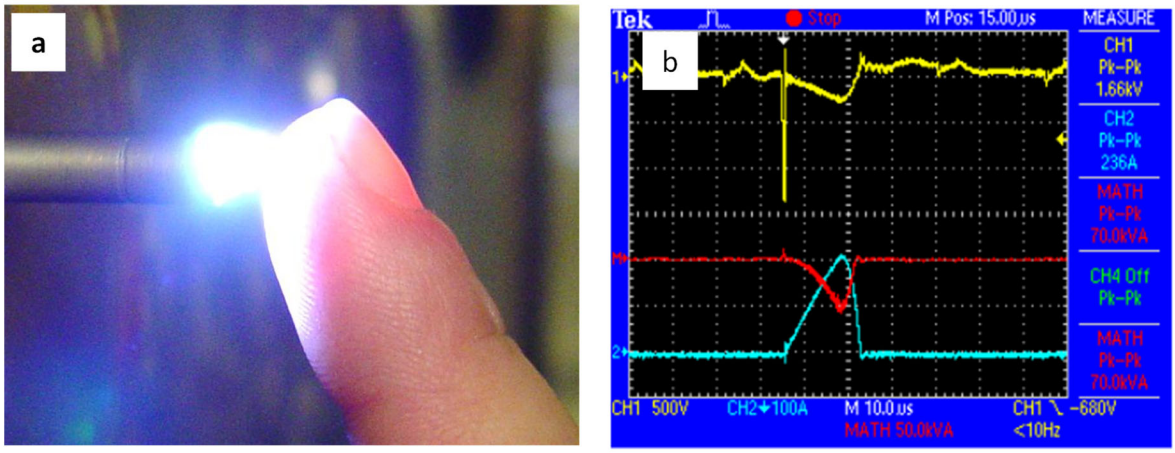

Figure 1. *(a) Photograph of HiPIPS Ar plasma demonstrating atmospheric, low temperature capability and (b) oscilloscope traces of voltage, current, and power during operation of HiPIPS.*

To overcome the vacuum chamber and high temperature processing, SwRI is developing a novel atmospheric pressure, non-thermal High Power Impulse Plasma Source (HiPIPS) technique for deposition of coatings (Figure 1). HiPIPS operates very differently from thermal plasma spray processes. The HiPIPS technology is an advanced variation of atmospheric pressure plasma process that allows for enhanced surface modification and deposition of functional coatings. The HiPIPS technology, consisting of an advanced pulsed DC generator in combination with atmospheric pressure plasma jets, provides an unparalleled plasma processing space of very high density and flux at low temperature and atmospheric pressure conditions. HiPIPS uses an inert carrier gas (e.g. N_2 or Ar) which flows, unheated, through the hollow cathodes to maintain a non-thermal plasma. The cathode is excited by pulse DC power and the free electrons enter into collisions with gas molecules. The inelastic collisions produce various reactive species (excited atoms and molecules, free radicals, etc.) which exit the source at high velocity. In this fashion, the surface is exposed to mainly active neutrals, radicals and ions, as opposed to kinetic particles. HiPIPS requires no external heating or cooling for operation. Preliminary results indicate that HiPIPS outperforms SOA ambient pressure non-thermal plasmas in areas such as power, current, precursor dissociation and flux, ion energy and precursor diversity, and rivals SOA vacuum plasma systems in many of these same categories. While still an early stage technology, HiPIPS has demonstrated, at proof-of-concept level, the ability to deposit durable coatings at ambient conditions. In this project, a variation of HiPIPS that employs a solid metal wire source material was further developed and investigated.

3.0 Materials and Methods

3.1 Technical Approach

In this project, SwRI conducted a comparative experimental study towards the development of atmospheric HiPIPS process for the deposition of field applicable and durable protective coatings. Towards this aim, four key technical tasks were identified. The overall approach is illustrated in Figure 2. A detailed description of the experimental design and work completed, along with technical progress and results, in relation to specific tasks is given below and in the following section, respectively.

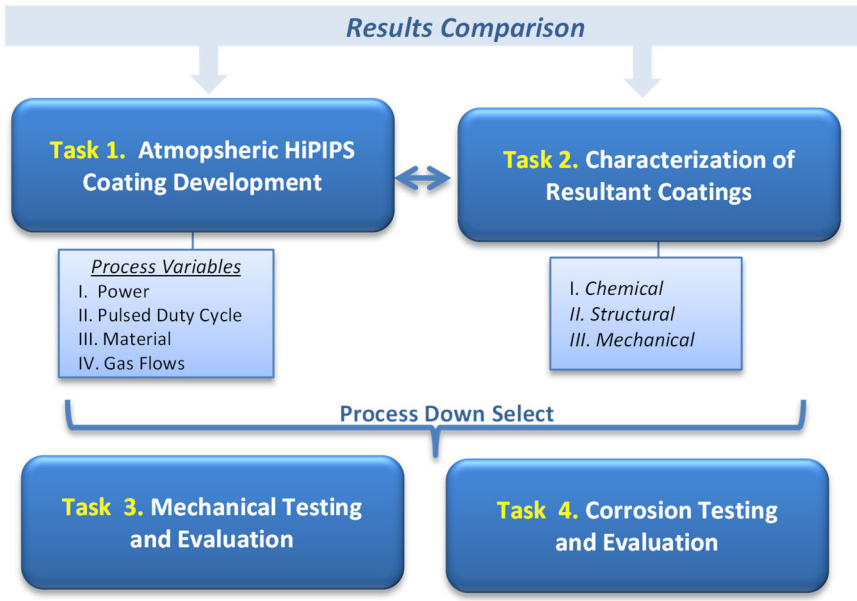

Figure 2. *Overall Program Plan.*

3.1.1 Task 1. Atmospheric High Power Impulse Plasma Source (HiPIPS)

The aim of this task was to develop atmospheric pressure HiPIPS device and process for deposition of durable protective coatings. A description of the materials and experimental methods conducted follows.

HiPIPS Design and Operation

A design for HiPIPS is schematically shown in Figure 3. The HiPIPS jet head fundamentally consists of a metal wire feed stock (the electrode), a metal tube, a ceramic tube and a metal nozzle. Metal wires were nominally 0.32 cm in diameter and metal tubes were nominally 1.2 cm in diameter and 4 cm in length. The metal wire was centered axially in the tube and the tip was positioned within ≤ 2 mm from the end of the nozzle. Driven by a pulsed DC power supply (Liaoning Beiyu Vacuum Science and Technology Co), the HiPIPS jet head was used at atmospheric pressure for various processes including plasma cleaning and deposition of metallic or ceramic coatings. The HiPIPS plasmas were operated in ambient room conditions without a controlled environment chamber. When the working gas is fed and DC pulses at certain peak voltage, frequency and pulse width are applied to the center electrode of the HiPIPS, plasma is generated between the electrode and the metal nozzle, resulting in the ablation of the electrode and the nozzle materials. As the DC pulse continues the current increases dramatically. Due to the high current capability of the advanced power supply design, extremely high peak power can be applied into the plasma within a short period of time. This high power discharge leads to the production of highly ionized gases. The advanced micropulsing capability of the power generator restricts discharge times to values below the time constant for instabilities.

Initially, we evaluated the feasibility of depositing coatings employing our original HiPIPS prototype head (Figure 4a). At the end of the first quarter, we designed and manufactured an advanced variation of the atmospheric pressure HiPIPS jet head, which utilizes polyvinyl alcohol (PVA) casing to reduce Fe contamination observed from the previous steel casing (Figure 4b).

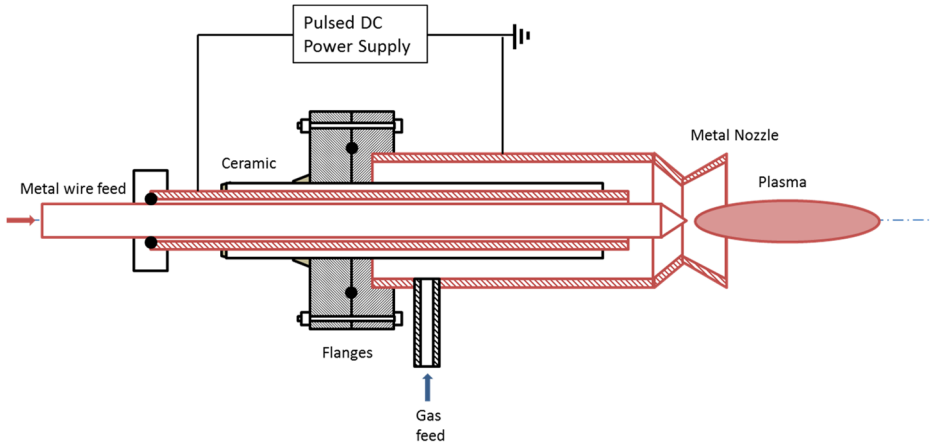

Figure 3. *Schematic of an atmospheric HiPIPS design for deposition of metallic films.*

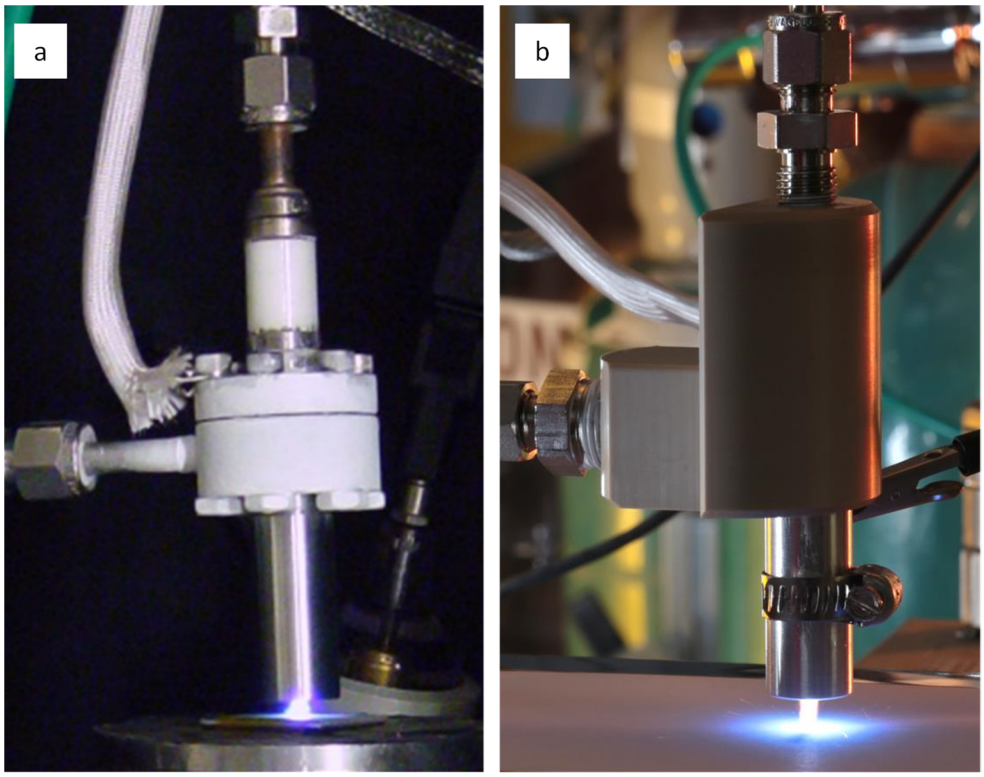

Figure 4. *Photographs of (a) the original prototype HiPIPS jet head and (b) an improved HiPIPS jet head developed and manufactured in the program.*

Plasma Characterization

Optical emission spectroscopy (OES) along with electrical and thermal probes were employed for measuring and calculating the plasma characteristics and their variation with systematic changes in HiPIPS process parameters and conditions. OES provides quantitative plasma diagnostics through measurement of optical emissions from excited states of species, usually formed by electron impact excitation of respective ground state species. An Ocean Optics HR4000CG-UV-NIR spectrometer fitted with a 3648-element linear-array charge-coupled device (CCD) detector provided high resolution ($\Delta\lambda$ = 0.75 nm) emission spectra throughout a 200 to 1000 nm wavelength range. All spectra were acquired through optical fiber at distance of 10 cm between the fiber aperture and the

plasma source. Absolute intensity calibrations were performed using two radiance calibration standards traceable to NIST. OES spectroscopic data were acquired without automatic noise subtraction and are shown herein without any numerical processing. The electrical properties of the HiPIPS plasma were studied by measuring the voltage and current transients across the discharge. The measurements were made using a high voltage probe (Tektronix P6015A) and an inductive current monitor (Pearsons Electronics Model 4418). The results were recorded on a digital oscilloscope (Tektronix).

Deposition Experiments

A number of depositions were carried out to study the effect of deposition parameters, such as pulse power and frequency, precursor gas, and deposition pressure, on the formation of thin films. We employed HiPIPS to generate metallic plasmas at atmospheric pressure using different source metal wires consisting of CoCr alloy, Ti-6Al-4V Titanium alloy, and Ti wires (0.125 in diameter). Table 1 shows the HiPIPS process parameters that were examined. The optimal operating range for HiPIPS during deposition was as follows. High purity Ar (99.995%) was used as the working gas and the flow rate controlled by a mass flow controller (MKS Instruments Model 247D) was varied from 3 to 20 slm. The pulsed voltage was varied from 0.6 to 2.5 kV, while the pulse frequency was fixed at 500 Hz with the pulse width fixed at 20 µs. In some experiments, nitrogen (N_2) gas was added in 1:1 ratio to Ar gas. Preliminary deposition experiments were performed on Si wafers. Initial deposition experiments were performed static, without substrate or plasma head movement. Upon verification of coating deposition on Si wafers, we sourced, installed and programmed a customized X-Y substrate rastering stage (shown in Figure 5). After deposition process parameters were set, deposition experiments were performed on 4340 steel and 7075 aluminum alloy substrates.

The distance between the plasma source and the substrate surface was set to approximately 8 mm. Standard silicon wafers (25 x 25 x 0.75 mm) and 4340 steel and 7075 aluminum alloy coupons (8 x 13 x 0.64 cm) (EMJ Metals, Earle M. Jorgenson Company) were used as substrates. Depositions were conducted using a customized X-Y substrate rastering stage. The films were deposited in multiple passes ranging from 3 to 10 passes at a scan velocity of 10 mm/s and a step size of 1mm. A negative bias ranging from 70 to 120 V was applied to the substrates during deposition. The 4340 steel substrates were mechanically polished to remove existing roughness and surface oxides. All substrates were solvent cleaned with isopropyl alcohol and air dried before deposition.

Table 1. *HiPIPS Process Parameters*

Process Parameters	Range
Peak Pulse Voltage	0.1 to 1.7 kW
Pulse Length	5 to 20 µsec
Pulse Frequency	0.1 to 1 kHz
Peak Pulse Current	10 to 400 A
Flow Rates	500 to 20000 sccm
Gas Species	Ar, N_2
Wire Material	CoCr, Ti, Ti-6Al-4V

Surface Preparation and Bond Layer Development

In addition to HIPIPS deposition process parameters, pre-cleaning with Ar plasma processing and bond layer treatments were evaluated. 4340 steel substrates were mechanically polished to remove existing roughness and rust. Samples were solvent cleaned with isopropyl alcohol. Bonding layer treatments evaluated including applying negative bias to the substrate and atmospheric pressure plasma processing using compressed air or hexamethyldisiloxane (HMDSO) gas precursors. Atmospheric pressure plasma using compressed air worked well to improve adhesion on Si wafer and stainless steel substrates. However, the atmospheric compressed air plasma caused the 4340 steel substrates to oxidize during treatment. We examined using an Ar and HMDSO atmospheric pressure plasma to form a nanometer thin bonding layer on the 4340 steel and 7075 aluminum alloy substrates. This bond layer worked to improve adhesion of HiPIPS coatings.

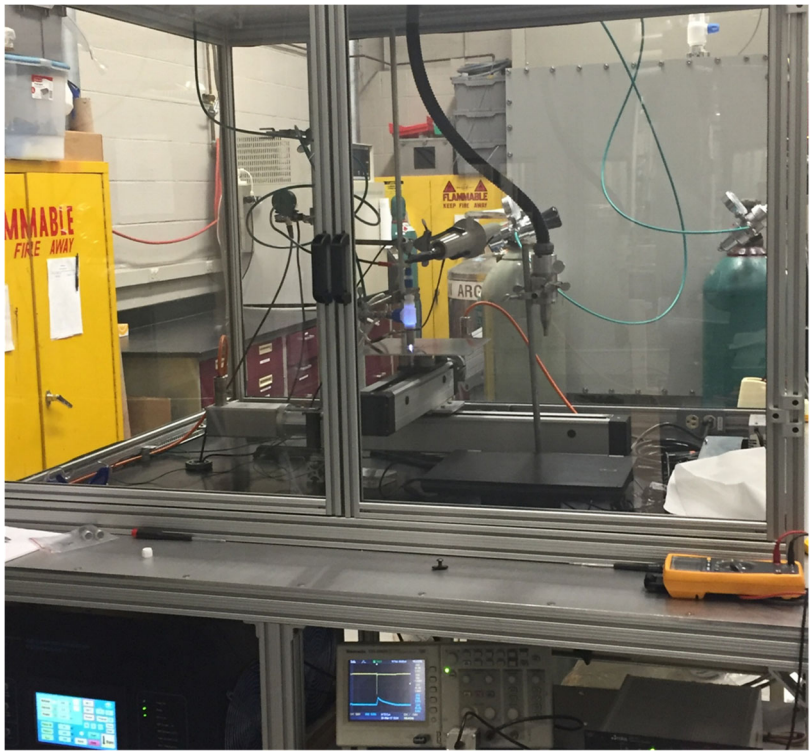

Figure 5. *Photographs of HiPIPS set-up with customized X-Y substrate rastering stage.*

Control Sample Preparation

Corpus Christi Army Depot (CCAD) provided chrome plating services, performed to CCAD Process Specification B-OO, to fabricate control samples for comparison testing in the project.

3.1.2 Task 2. Characterization of Resultant Coatings

The main focus of this task was to characterize the structural, chemical, and mechanical properties of the resultant HiPIPS coatings. This task is logically linked to and was performed in parallel with Task 1. The characterization results were used for iterative deposition process development. The following outlines characterization methods conducted.

Scanning electron microscopy (JEOL 5800LV SEM) was used for microstructural examination of the resultant coatings. Cross sectional samples were examined to determine the composition of the interface layer and its effect on coating adhesion. Energy-dispersive X-ray (EDX) spectroscopy along with EDX mapping was used to determine film elemental composition. The coating adhesion was examined using standard tape test per ASTM D3359-02. The nanohardness of HiPIPS thin films

were obtained by nanoindentation technique (Hysitron Triboscope, USA). Load controlled indentation testing followed a trapezoidal loading profile with a hold time of typically 10 s at peak load. Peak loads were ranged from 3000 to 5000 μN. The diamond indenter was a Berkovich tip with a tip radius of 100 nm. X-ray Diffraction (XRD) analysis was carried out on the surface of the as-deposited samples using a Siemens KRISTALLOFLEX 805 XRD in a Bragg-Brentano configuration (CuKα radiation generated at 40 kV and 25 mA). All the patterns were recorded between 20 and 80° (2θ) at steps of 0.05°.

3.1.3 Task 3. Mechanical Testing and Evaluation

The objective of this task was to perform stress-life (S-N) tests on baseline and HiPIPS coated alloys in order to assess the effect on the fatigue performance. In addition to characterizing the fatigue performance, the failure modes will also be documented to aid in understanding the influence, if any, that these surface treatments have.

Material and Specimen Geometry

The alloy selected for this effort was 4340 heat-treated to an ultimate strength of near 200 ksi (based on a hardness evaluation). Round bar stock having a diameter of 1 in. was used for coupon fabrication.

A dog-bone based fatigue geometry was selected that integrated into test fixtures already available at SwRI's Solid and Fracture Mechanics Laboratory. The geometry is presented in Figure 6. Overall, the coupon included threaded ends that secured into female threaded grips and a gage section diameter of 0.25 in. Furthermore, the gage section of the coupon was longitudinally polished to achieve a consistent surface finish and minimal residual stress as is critical in fatigue life testing. Each coupon was given an identification label in the format of SN-*XX* where *XX* was numbered 1 through 50. Prior to testing, the diameter of each coupon was measured using an optical traveling microscope; a contact measuring method was not used due to potential concerns with surface damage that may occur.

Test Method

Constant-amplitude load-controlled fatigue testing was performed per ASTM E466. A servohydraulic test frame was utilized to apply the constant amplitude loading of the coupons. A stress ratio (ratio of minimum load to maximum load) of 0.1 was used during testing with a cyclic rate of 10 Hz. Prior to testing, the frame alignment was verified with a target of <5% bending. In addition, a universal joint was used in the load-train to mitigate any bending associated with misalignment.

Testing was performed in laboratory ambient conditions, namely 72 °F and 30-50%. Testing concluded upon specimen failure or reaching a runout life (5 million cycles). Data recorded included the specimen identification, specimen condition, loading levels, cycles to failure, and failure location/mode. In addition, typical S-N plots and bar charts were prepared to graphically present the data.

Using baseline coupons, a maximum cyclic stress of 155 ksi was chosen for this focused investigation. The resulting fatigue life at this cyclic stress condition was near 100,000 cycles. A total of three baseline coupons were tested at 155 ksi while a minimum of five coupons were tested for each surface treatment.

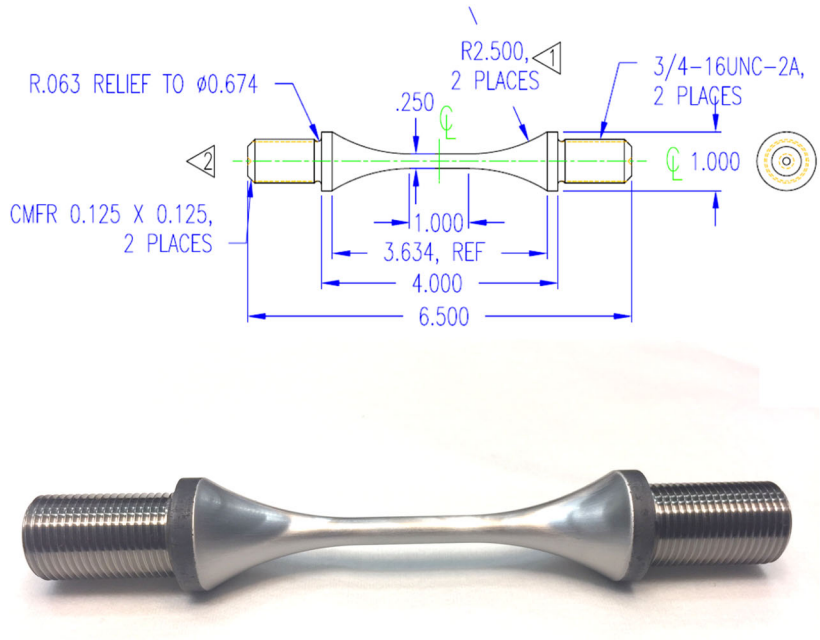

Figure 6. *Schematic and photograph of S-N dogbone specimens for mechanical testing.*

3.1.4 Task 4. Corrosion Testing and Evaluation

The corrosion resistance of the deposited coatings were examined in this task and compared to coatings deposited using traditional coating methods (i.e. electrolytic chrome plating). Control substrates coated using traditional methods (Cr plating) were obtained from the CCAD. The atmospheric corrosion performance of these coatings were evaluated by exposing coated panels to the GM 14872 accelerated corrosion test environment. Growing evidence indicates that this test more closely replicates field corrosion than other commonly used accelerated testing protocols, and previous SERDP projects to find alternatives to chrome plating have used this corrosion test.

4.0 Results and Discussion

4.1 Results Summary

The following sections provide a summary of main results and progress.

4.1.1 HiPIPS Plasma Process Space Investigations

The first half of the project focused on the assembly, development and qualification of HiPIPS system followed by experiments where the process parameters were systematically varied to examine their effects of the resulting HiPIPS plasma. HiPIPS investigations (over 50 experiments with argon gas and Ti, CoCr, and Ti-6Al-4V wires) confirmed our hypothesis that high peak power pulses can be achieved (10-70 kW) resulting in high peak currents (100 - 250 A) and increased ionization and plasma density while maintaining low overall power (40W) and substrate processing temperatures (<50 °C). Shown in Figure 7 are snap shots of the oscilloscope screen exhibiting the voltage, current and power in a pulse for the HiPIPS running on (a) Ti-6Al-4V electrode and nozzle and (b) CoCr electrode and nozzle. The typical high peak currents and high peak powers in the pulse can be observed. Other parameters such as the peak voltage, pulse frequency and pulse width can be seen on the oscilloscope readouts.

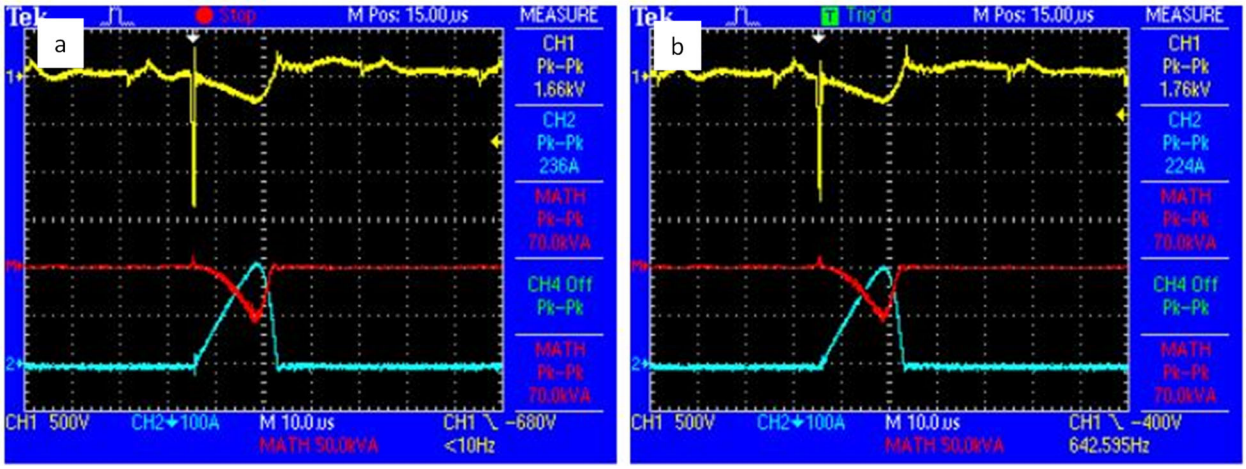

Figure 7. *Oscilloscope traces of voltage, current and power during the operation of the HiPIPS with Ar and (a) Ti-6Al-4V electrode and nozzle and (b) CoCr electrode and nozzle.*

OES measurements were used for detection of excited state species in the plasma, and their variation with systematic changes in HiPIPS process parameters and conditions. OES provides quantitative plasma diagnostics through measurement of optical emissions from excited states of species, usually formed by electron impact excitation of respective ground state species.

Figure 8 shows the optical emission spectra measured for HiPIPS plasma with a Ti wire interacting with Ar gas. The vertical axes of the figures indicate the number of photons or intensity. All spectra are shown as measured without noise subtraction or software processing. A number of atomic line are clearly observed. The lines observed in the 690 - 820 nm range are characteristic of Ar in both wavelength and relative intensities. The lines observed in the 320 - 670 nm range are assigned to Ti I and Ti II. Moreover, the high relative intensity and common transition probability for Ti I line at wavelength $\lambda = 521$ nm and the Ti II line at wavelength $\lambda = 670$ nm are present [8]. From, the inset photograph we can clearly see the bright plasma characteristic of high ion density of HiPIPS.

The metallic emission line intensities results from a two-step process. First, metallic atoms (Ti, Co, Cr, Al) are sputtered from the wire by Ar ions:

$$Ar^{+} + \text{Metal Wire} \Rightarrow M^{+*} \qquad (1)$$

Second, these sputtered species are excited either by secondary electrons to form metal excited states:

$$M+ + e^{-1} \Rightarrow M^{*} \qquad (2)$$

Thus, the OES spectral measurements confirm the presence of Ti^{*} and Ti^{+*} with high phonon intensities in HiPIPS plasma.

Figure 9 shows the optical emission spectra measured for HiPIPS plasma with a Ti-6Al-4V wire interacting with Ar gas. The characteristic Ar lines in the 690 - 820 nm are observed again. Yet, of more interest are that the spectral lines in the metallic region of the 320 - 670 nm range differ from the spectra of the HiPIPS Ti wire-Ar plasma. The strongest emission lines are still located in the 320 - 670 nm region are still assigned to Ti I and Ti II transitions. However, new lines are present for Al and V, such as Al I line at wavelength $\lambda = 400$ nm and the V I line at wavelength $\lambda = 420$ nm are present. [8].

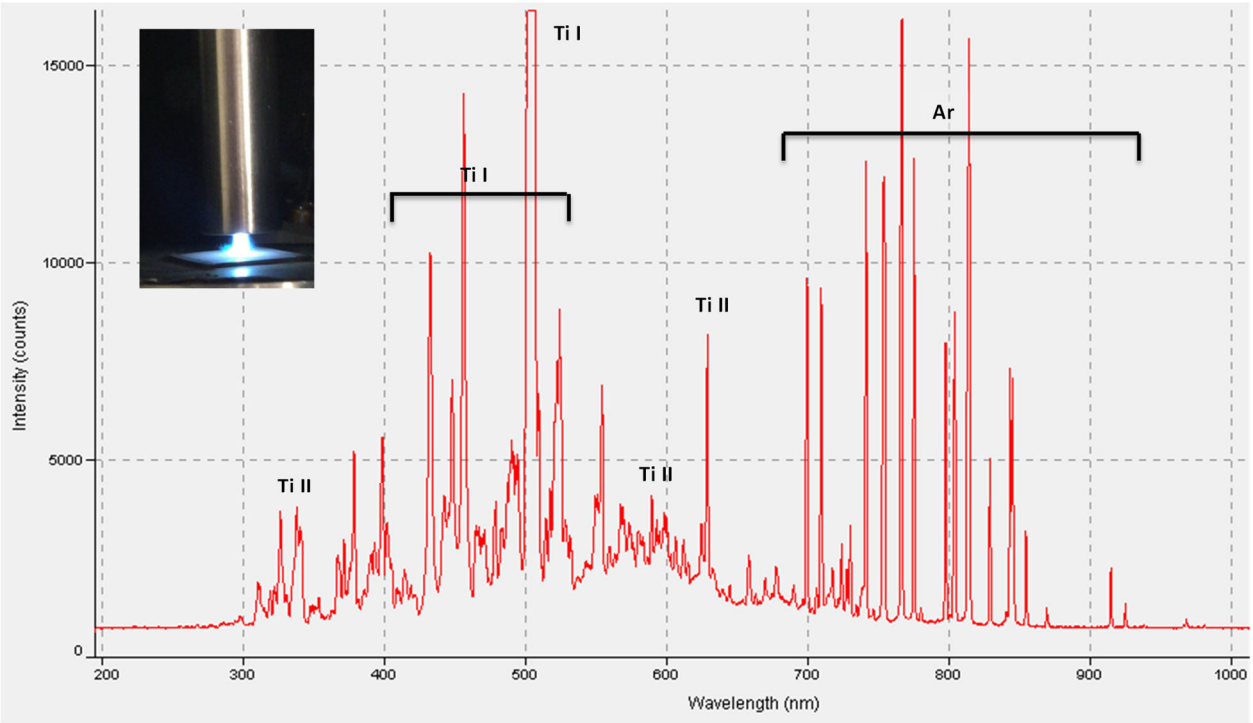

Figure 8. *Optical emission spectrum and photograph (inset) during the operation of the HiPIPS with Ar and Ti electrode and nozzle.*

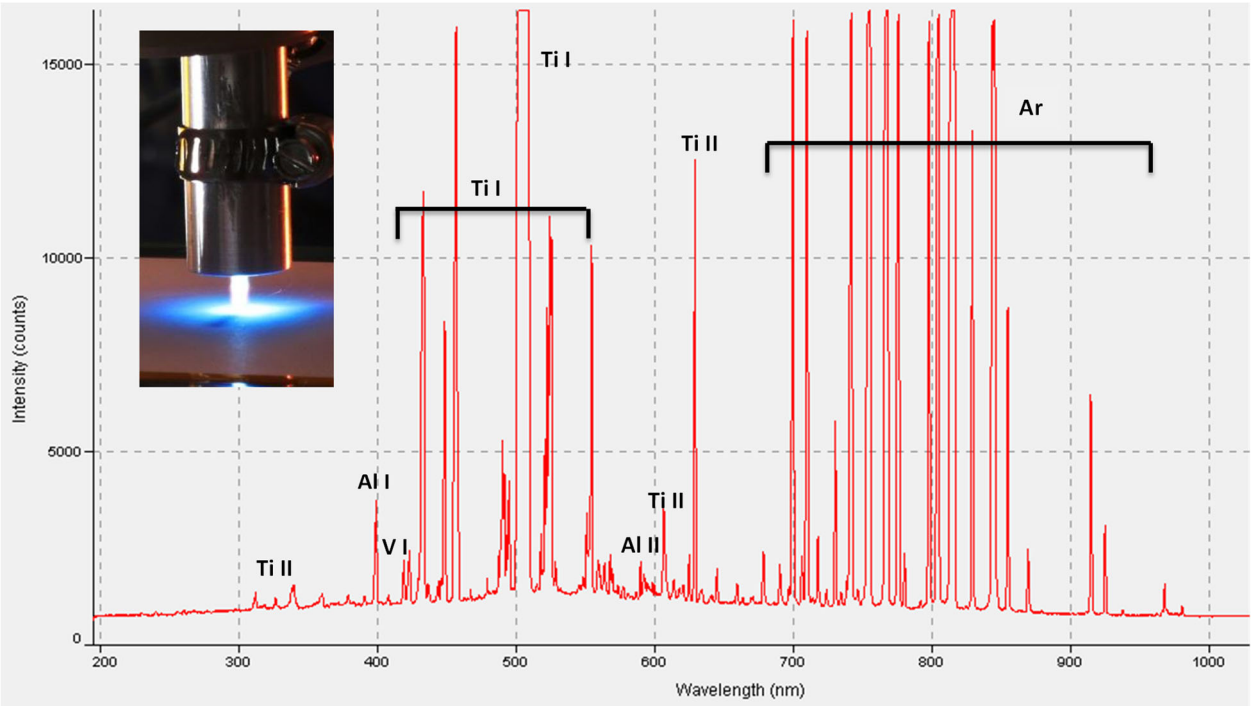

Figure 9. *Optical emission spectrum and photograph (inset) during the operation of the HiPIPS with Ar and Ti-6Al-4V alloy electrode and nozzle.*

Shown in the inset of Figure 10 is a photograph of HiPIPS in operation with Ar and CoCr wire electrode. Corresponding optical emission spectra is presented in Figure 10. Spectral lines in the 690 - 820 nm range are again characteristic of Ar. The strongest emission line at wavelength λ = 525 nm is for Cr I. Other numerous Cr I and Cr II lines are present in the 220 - 550 nm range. Also present are atomic lines for Co I in the 320-375 nm region and at wavelengths λ = 575 and 612 nm [8]. Of note are that there are no lines which could be assigned to higher (n>2) ionization states for Cr. Therefore, the OES measurements verify the absence of any hex-Cr in HiPIPS CoCr plasma.

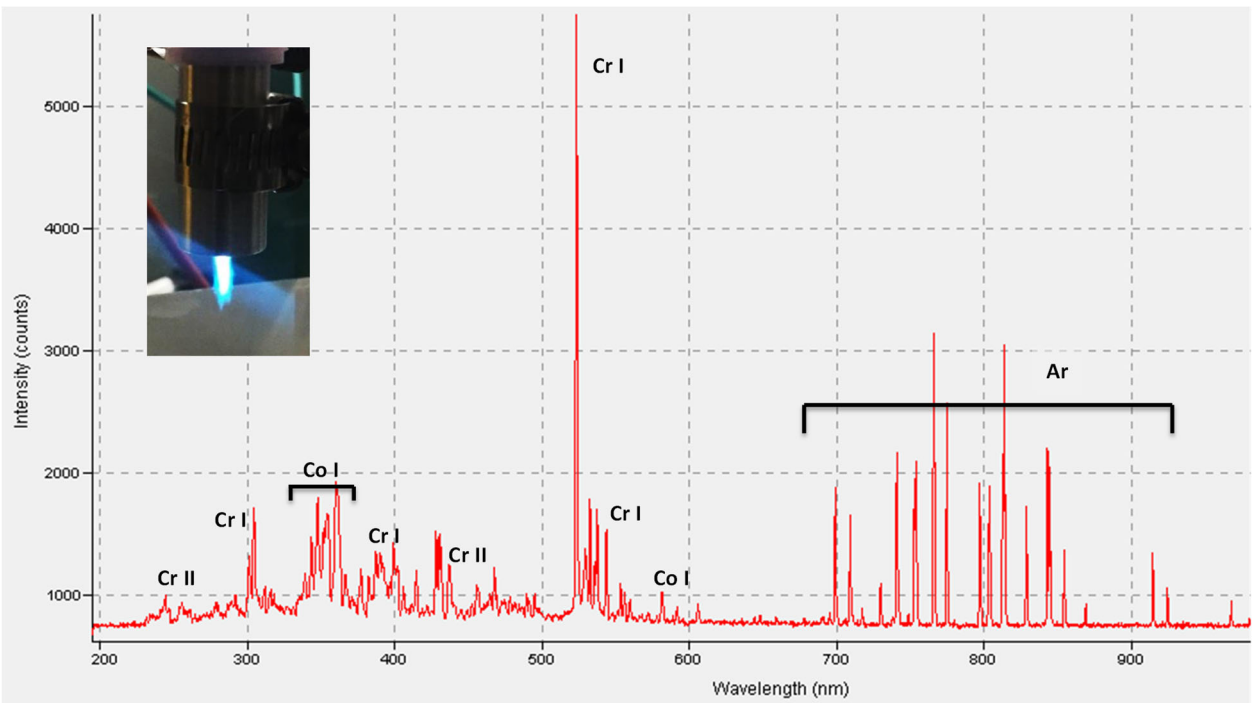

Figure 10. *Optical emission spectrum and photograph (inset) during the operation of the HiPIPS with Ar and CoCr alloy electrode and nozzle.*

Figure 11 presents the optical emission spectrum during the operation of HiPIPS with Ar and N_2 gases at a 1:1 ratio with a Ti electrode. The characteristic Ar lines normally obviously evident in the 690 - 820 nm region are not observed. From the 310 to 410 nm region, several emission molecular bands are detected and attributed to the N_2 and N_2^+ species. The three emission lines from 742 to 747 nm are attributed to atomic N. Also present are several Ti atomic lines, including the characteristic Ti I line at wavelength λ = 521 nm and the Ti II line at wavelength λ = 670 nm. The absence of the Ar lines can be described by interactions between Ar and N_2 gases. Timmermans et. al suggests that in this kind of discharge, N_2^+ results from charge transfer reaction involving Ar^+ energetic ions [9].

$$N_2 + Ar+ \Rightarrow N_2^+ + Ar \qquad (3)$$

The presence of energetic electrons could further initiate dissociation, ionization and excitation processes in the plasma. Where, N_2^+ may be responsible for atomic N formation.

$$N_2^+ + e^{-1} \Rightarrow N + N \qquad (4)$$

Altogether, the OES spectra have successfully detected and identified charged state of the excited species in the plasma that will ultimately form the resultant deposition coatings.

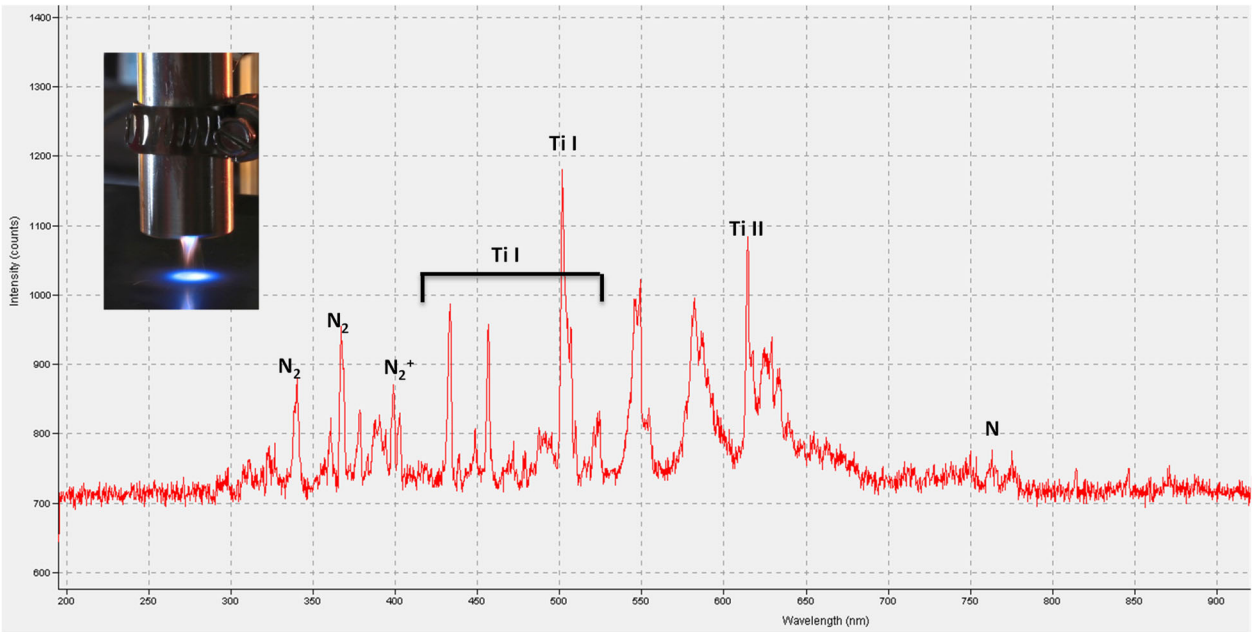

Figure 11. *Optical emission spectrum and photograph (inset) during the operation of the HiPIPS with Ar and N_2 and Ti electrode and nozzle.*

4.1.2 HiPIPS Deposition Experiments

Initial HiPIPS deposition experiments were carried out statically (no movement of substrate or HiPIPS head on Si (100) wafer and stainless steel (SS304) coupons (1 in x 2 in). With this setup, deposition trials were conducted on the samples using HiPIPS under various process conditions (shown in Table 1) to optimize the deposition rate, chemistry, uniformity and thickness of the coatings. Upon verification of coating deposition on Si wafers, we conducted dynamic deposition studies using a customized X-Y substrate rastering stage. Figure 12 presents photographs of exemplary HiPIPS Ti-6Al-4V deposition studies under initial static and then dynamic conditions.

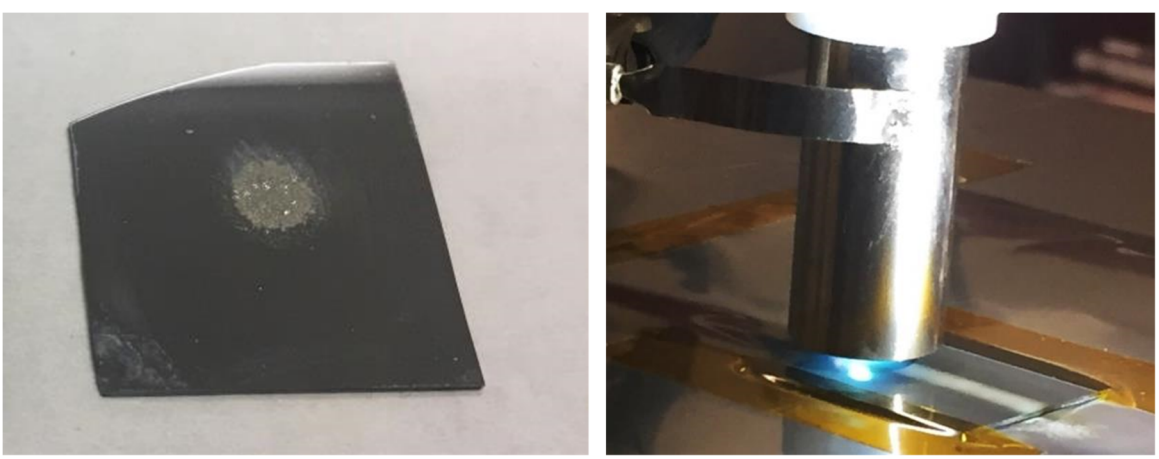

Figure 12. *Photographs depicting the evolution of preliminary HiPIPS deposition studies from static to dynamic on Si wafer substrates. Both exemplars shown are Ti-6Al-4V depositions.*

Interestingly, we discovered that under HiPIPS process parameters using low voltage bias (< 0.3 kV), static (no substrate or head movement) and no substrate bias (substrate at ground) yielded the formation of metallic nanoparticles in lieu of deposition of a coating. Whereas, HiPIPS process space using higher bias voltage, dynamic movement of substrate and bias voltage of at least - 40 V resulted in film or coating deposition. Figure 13 presents exemplary SEM images that depict the difference in deposit morphologies resulting from varying HiPIPS process conditions. These results indicate that a variation of process conditions can modify the deposit morphology from spherical nanoparticles towards that of a coating. The one-step synthesis of metallic nanoparticles using HiPIPS is an interesting discovery that may have utility in other project investigations and applications.

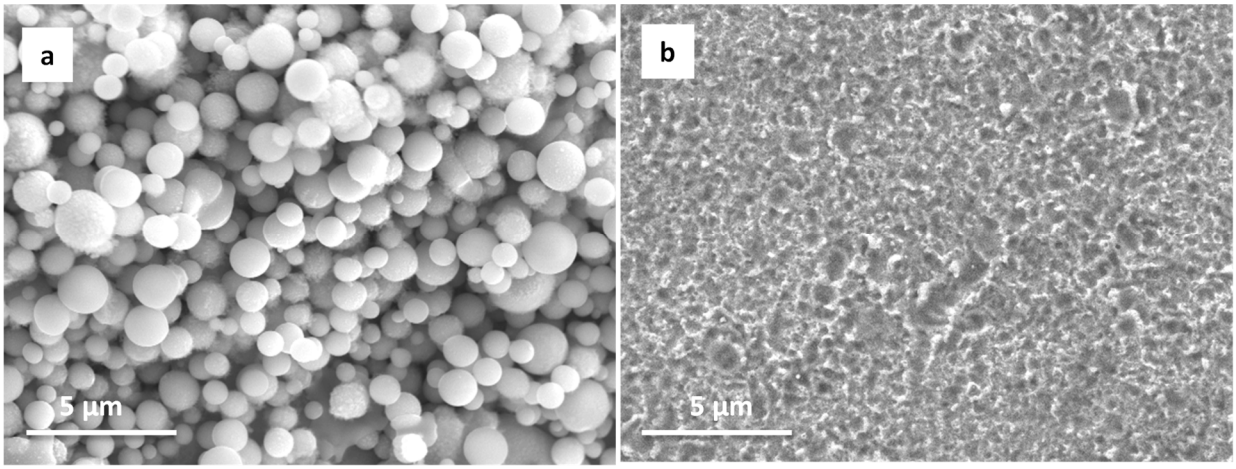

Figure 13. *SEM images of resultant deposits from two HiPIPS Ti-6Al-4V deposition experiments that depict how variation of HiPIPS process conditions can modify the result from synthesis of spherical nanoparticles towards deposition of a coating.*

We then conducted deposition trials of AP-HiPIPS CoCr, Ti-6Al-4V, Ti and TiN coatings and characterized the resulting coatings with SEM and EDS. A cross-section SEM image of HiPIPS CoCr coating on Si wafer is shown in Figure 14.

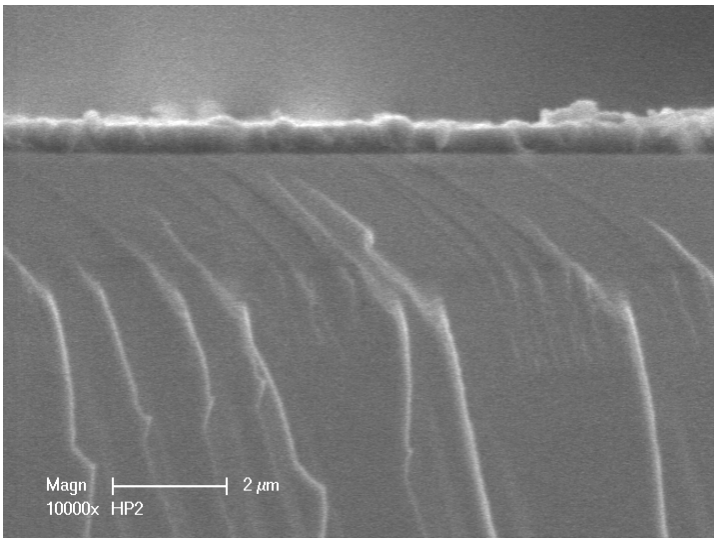

Figure 14. *Cross-section SEM image of a HiPIPS CoCr coating on Si wafer.*

After successful HiPIPS CoCr coating development experiments on Si wafer, we conducted deposition trials on steel substrates. HiPIPS Ti-6Al-4V and CoCr alloy coating deposition process conditions on 4340 steel substrates were developed through a series of trials where a pulsed voltage range of 0.6 - 2.5 kV with the pulse frequency fixed at 500Hz and the pulse width fixed at 20 µs, a flow rate of 15 slm of Ar, and a substrate bias range of 70 to 100 V were utilized. To get to a uniform coating surface coverage it required at least 8 passes or coating layers. Shown in Figure 15 is a cross-section SEM micrograph and corresponding EDS elemental maps representative of HiPIPS CoCr coating. As can be observed in the SEM image, the coating remains adhered after machining and polishing the 4340 steel substrate. Typical coating thickness varied from 1 to 5 µm depending on deposition time. The average deposition rate was approximately 64 nm/sec. EDS mapping analysis reveals that the coating layer contains high amounts and uniform distributions of chromium and cobalt. The elemental composition of the resultant coating can be correlated to the excited species observed in the OES spectra of the HiPIPS CoCr plasma. Likewise, shown in Figure 16 is a cross-section SEM micrograph and corresponding EDS elemental maps of HiPIPS Ti-6Al-4V coating. The Ti-6Al-4V coating also remains adhered after machining and polishing the 4340 steel substrate. The EDS elemental maps reveal that the coating layer contains uniform distribution and high amounts of Ti, Al, and V. The elemental composition of the resultant coating can be correlated to the excited species observed in the OES spectra of the HiPIPS Ti-6Al-4V plasma.

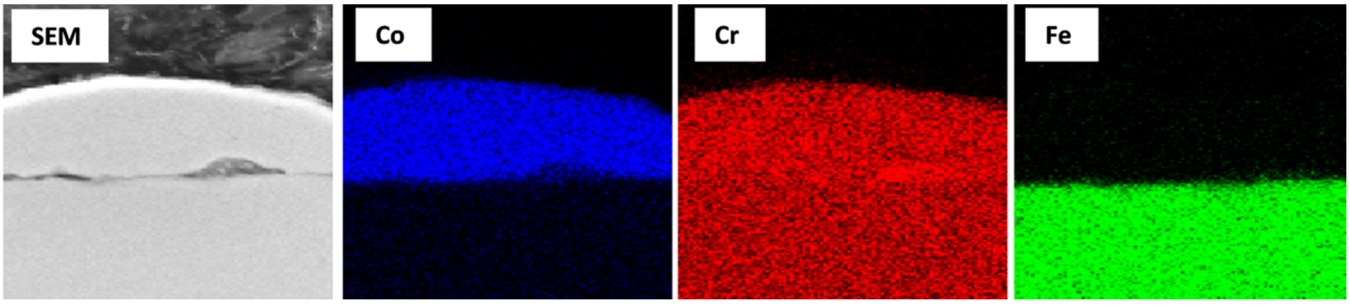

Figure 15. *Cross-section SEM micrograph (left) and corresponding EDS elemental maps of HiPIPS CoCr coating on 4340 steel substrate. EDS mapping analysis reveals coating layer contains uniform distribution and high amounts of cobalt and chromium.*

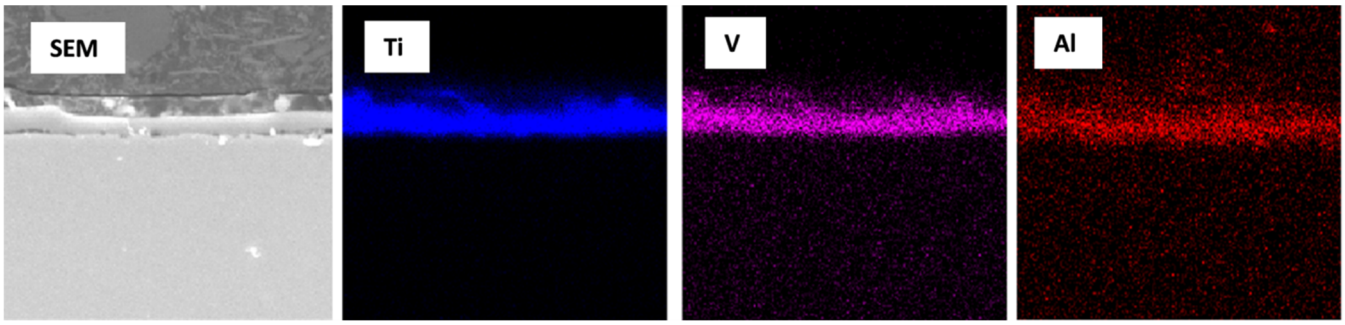

Figure 16. *Cross-section SEM micrograph (left) and corresponding EDS elemental maps of HiPIPS Ti-6Al-4V coating on 4340 steel substrate. The coating remains adhered after machining and polishing. EDS mapping analysis reveals that the coating layer contains uniform distribution and high amounts of titanium, vanadium and aluminum.*

We also conducted deposition trials towards a TiN coating using HiPIPS with pure Ti electrode and nozzle and addition of nitrogen gas to argon gas. Using pure nitrogen gas would result in only N_2 plasma and no coating deposition without energetic Ar ions to sputter the wire electrode. We systematically varied the ratio of Ar and N_2 and settled on a ratio of 1:1 for deposition trials.

Figure 17 compares photographs of as deposited coatings on Si wafers from deposition process using the HiPIPS with pure Ti electrode with Ar gas only and with Ar and N_2 gas at 1:1 ratio. The coating resulting from HiPIPS operation with pure Ti electrode with Ar results in coating with a silver and white color. The white comes from oxidation of the depositing Ti at ambient conditions, as Ti is a known oxygen getter material. The coating resulting from HiPIPS operation with pure Ti electrode with Ar and N_2 gas has more of the characteristic goldish color of TiN coating. Shown in Figure 18 is the EDS data of the HiPIPS deposition on Si wafer using Ti electrode with Ar. Note that oxygen is indeed observed in the elemental composition of the film corroborating the qualitative white color evidence of titanium oxide. Shown in Figure 19 is the EDS data of the HiPIPS deposition on Si wafer using Ti electrode with Ar and N_2. Note that nitrogen is indeed observed in the elemental composition of the film.

A representative XRD spectrum of the as-deposited HiPIPS film on stainless steel substrate using Ti electrode with Ar and N_2 gas at 1:1 ratio is shown in Figure 20. The diffraction peaks related to different crystalline planes of titanium nitride are observed. The spectrum is characterized by the presence of peaks at $2\theta = 38.6^o$, 43.6^o and 65.2^o which correspond respectively to the (111) and (200) planes of TiN thin films. Titanium nitride diffraction peaks are in agreement with the Joint Committee for Powder Diffraction Standards (JCPDS) standard data (JCPDS card number 38-1420 and JCPDS card number 23-1458).

The nanohardness of HiPIPS thin films were obtained by nanoindentation technique (Hysitron Triboscope, USA). Load controlled indentation testing followed a trapezoidal loading profile with a hold time of typically 10 s at peak load. Peak loads were ranged from 3000 to 5000 μN. The diamond indenter was a Berkovich tip with a tip radius of 100 nm. The hardness of HiPIPS TiN, Ti6Al4V and CoCr films ranged from 11.56 to 14.09, 3.92 to 4.44, and 6.20 to 8.42 GPa, respectively.

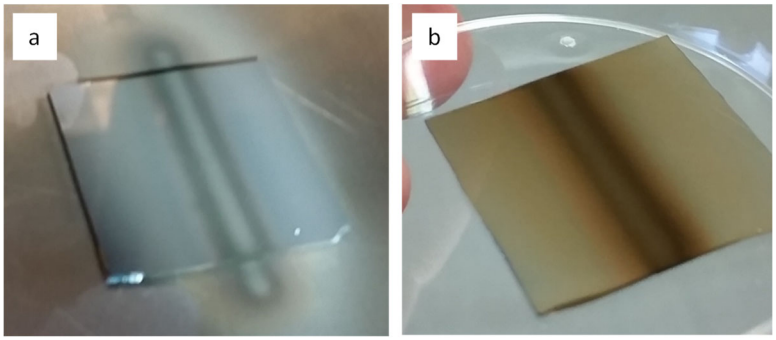

Figure 17. *Photographs of as deposited coating from deposition processes using the HiPIPS with pure Ti electrode and (a) Ar gas only and (b) Ar and N_2 gas at 1:1 ratio.*

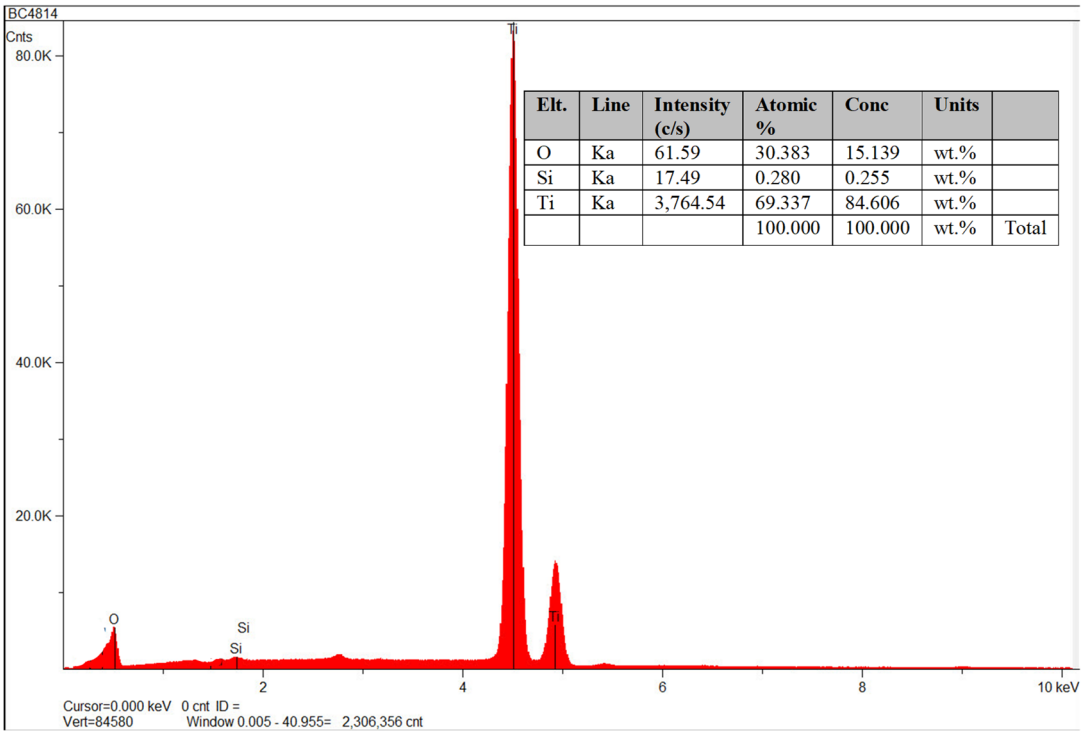

Elt.	Line	Intensity (c/s)	Atomic %	Conc	Units	
O	Ka	61.59	30.383	15.139	wt.%	
Si	Ka	17.49	0.280	0.255	wt.%	
Ti	Ka	3,764.54	69.337	84.606	wt.%	
			100.000	100.000	wt.%	Total

Figure 18. *EDS data of the deposited coating (shown in Figure 17a) from operation of HiPIPS with pure Ti electrode and Ar.*

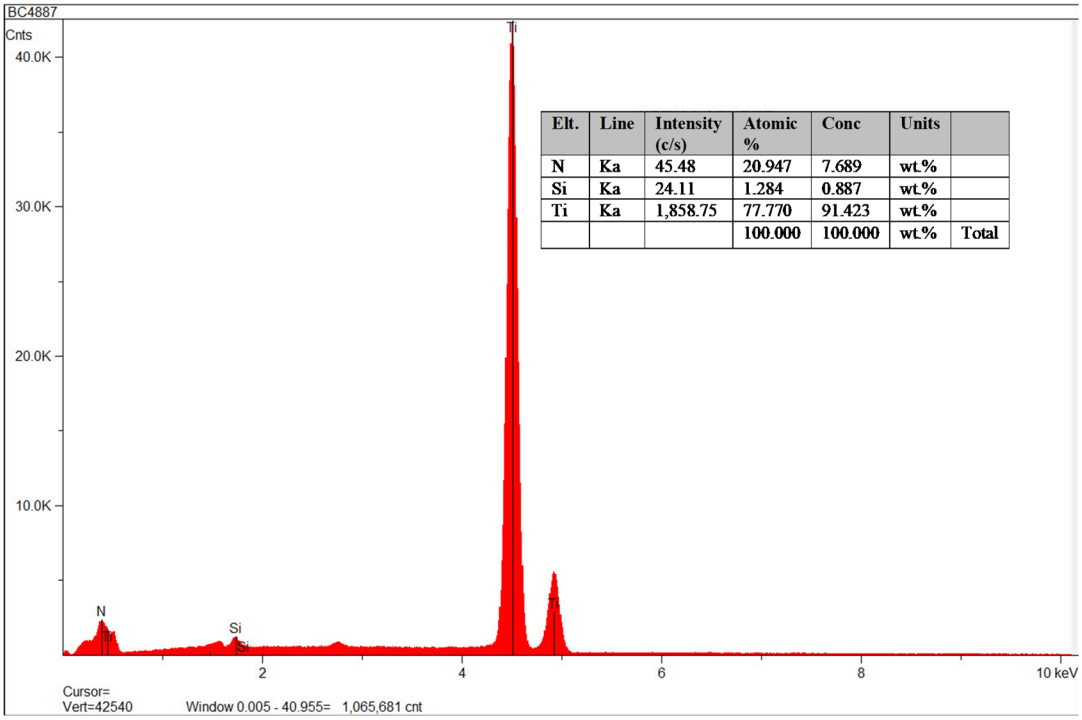

Elt.	Line	Intensity (c/s)	Atomic %	Conc	Units	
N	Ka	45.48	20.947	7.689	wt.%	
Si	Ka	24.11	1.284	0.887	wt.%	
Ti	Ka	1,858.75	77.770	91.423	wt.%	
			100.000	100.000	wt.%	Total

Figure 19. *EDS data of the deposited coating (shown in Figure 17b) from operation of HiPIPS with pure Ti electrode and 1:1 of Ar:N_2.*

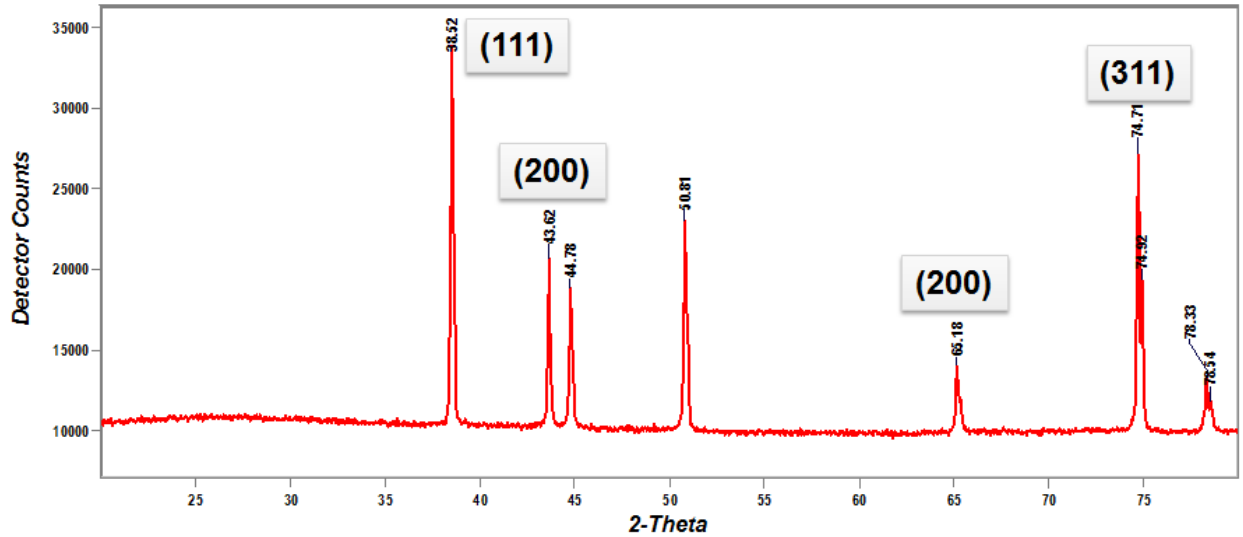

Figure 20. *XRD of the as-deposited HiPIPS coating using Ti electrode and 1:1 ratio of Ar:N_2.*

4.1.3 Control Sample Preparation

CCAD provided chrome plating services to fabricate control and baseline samples for comparison testing in the project. CCAD chrome plated tensile dogbone specimens and corrosion testing panels provided by SwRI (Figure 21). The plating thickness was 1.0 to 2.0 mils thick, and all plating procedures and related steps (e.g. relief baking and surface preparation) were performed to CCAD Process Specification B-OO.

Figure 21. *Photograph of exemplary Cr-plated 4340 steel dogbone tensile specimens and 4340 steel corrosion test panels obtained from CCAD.*

4.1.4 Corrosion Testing and Evaluation

SwRI completed GMW 14872 testing on coated and uncoated 4340 steel samples. The coatings tested include the SwRI-developed atmospheric plasma coatings as well as coatings applied using conventional plating techniques and uncoated samples for comparison. All steel coupons exhibited significant amounts of corrosion after 15 cycles of testing, including the conventionally plated samples. The atmospheric plasma-applied Ti6Al4V and CoCr coatings on steel substrates showed more corrosion damage than the conventional coatings, but significantly less than that of the uncoated sample (Figure 22). All steel coupons were removed from the chamber after 15 cycles of testing.

SwRI also completed GMW 14872 testing on SwRI-developed HiPIPS CoCr coatings, SwRI HiPIPS SiOx bond layer coating, conventional Cr plating techniques (CCAD plating), and uncoated samples 7075 aluminum alloy samples for comparison. Aluminum coupons were tested for 42 cycles, longer than the 15 cycles for the steel coupons because the coatings on the aluminum coupons were less affected by the cyclic test. The uncoated samples showed significant damage at the completion of this testing. The HiPIPS CoCr coating and HiPIPS organosiloxane base layer alone (< 200 nm) coatings performed better than the samples plated with the conventional coatings and the uncoated samples (Figure 23).

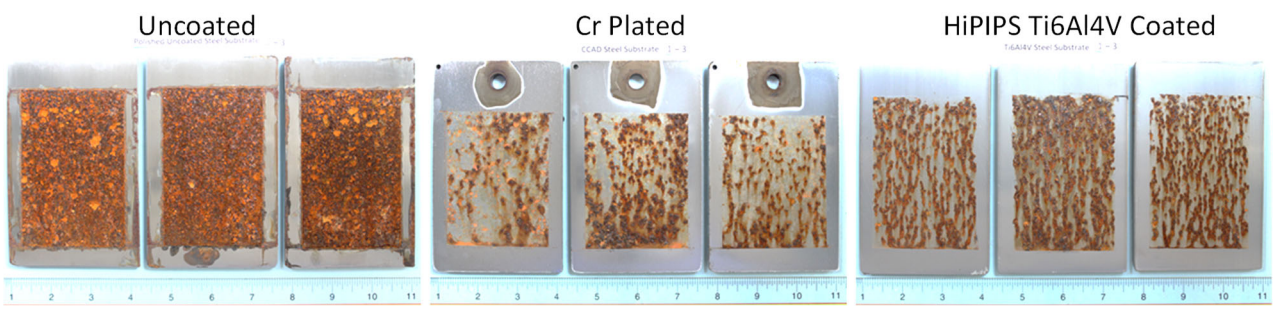

Figure 22. *Photographs of samples after 15 cycles of GMW 14872 testing on 4340 steel substrates. The coatings tested included the SwRI-developed HiPIPS coatings as well as coatings applied using conventional plating techniques and uncoated samples for comparison.*

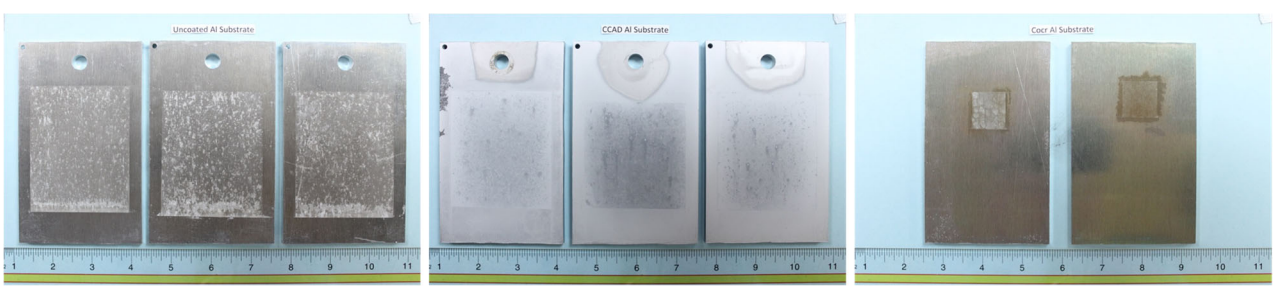

Figure 23. *Photographs of samples after 42 cycles of GMW 14872 testing on 7075 aluminum alloy substrates. The coatings tested included the SwRI-developed HiPIPS coatings as well as coatings applied using conventional plating techniques and uncoated samples for comparison.*

4.1.5 Mechanical Testing and Evaluation

The focus of this mechanical test effort was to investigate to influence of the surface treatment methods on the fatigue performance of the substrate material. While the application of surface coatings or treatments can enhance wear or corrosion resistance, it can also influence the fatigue performance, and as such it is important to characterize how the material responds under cyclic loading. Baseline fatigue performance was compared to three surface treatments that included: CCAD Cr plated, SwRI HiPIPS Ti6Al4V and SwRI HiPIPS CoCr (Figure 24). Comparison of fatigue performance was based on a maximum stress level of 155 ksi which provided finite fatigue lives for all conditions.

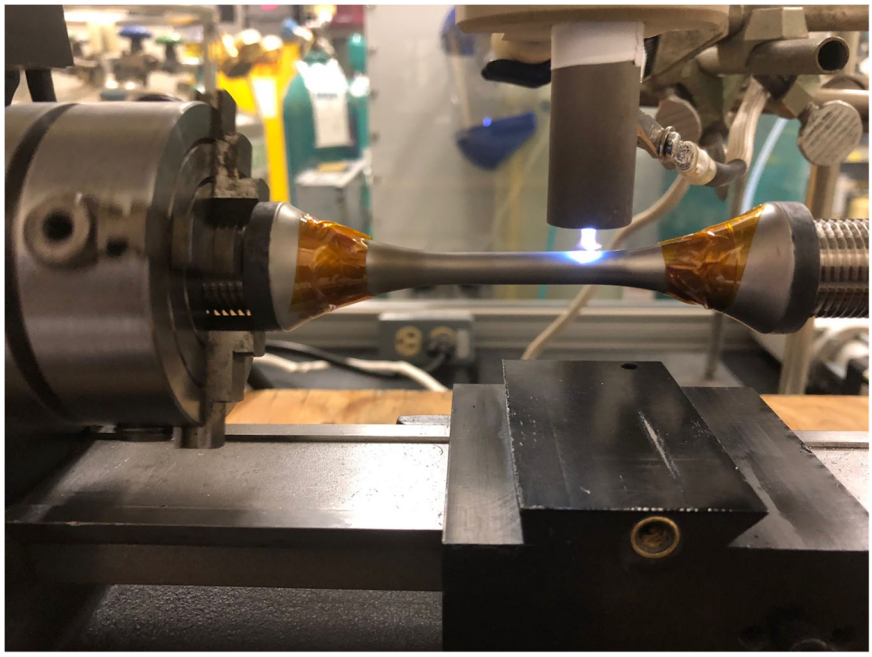

Figure 24. *Photograph of HiPIPS Ti6Al4V deposition process on dog-bone fatigue sample specimen. The HiPIPS plasma head remained stationary as the dog-bone specimen was translated and rotated during the deposition process.*

A tabular summary of the fatigue stress-life results is presented in Table 2. In addition, a bar-chart is presented in Figure 25 for the test results at 155 ksi max stress for all conditions evaluated.

When comparing the three surface treatments, there appears to be three distinct groups of fatigue lives. The HiPIPS Ti6Al4V had the highest fatigue life followed by the HiPIPS CoCr and the CCAD condition demonstrating the lowest fatigue life. When comparing the baseline response, the HiPIPS Ti6Al4V had a similar stress-life response. The CCAD Cr Plated, on the other hand, was approximately an order of magnitude shorter in life. The SwRI HiPIPS CoCr was approximately half the fatigue life of the baseline conditions. When visually evaluating the fracture surfaces of the failed coupon, surface crack initiation followed by crack growth was the mode of failure. It is important to note that the CCAD condition demonstrated numerous surface cracks along the gage length with one of those cracks becoming the dominant crack and cause of failure. Recall the CCAD condition had an order of magnitude reduction in life compared to the baseline. This high population of surface cracks supports the significant reduction in life.

Table 2. *Summary of stress-life test results.*

Condition	Specimen	Dia.	Area	Max Load	Max Stress	Cycles to Failure	Comments
Baseline	SN-27	0.252	0.049851	7.50	150	63820	OD initiation
	SN-26	0.2505	0.049259	7.80	158	89268	OD initiation
	SN-25	0.2525	0.050049	7.80	156	120046	OD initiation
	SN-42	0.252	0.049851	7.80	156	167848	OD initiation
	SN-22	0.2515	0.049653	8.20	165	62692	OD initiation
	SN-8	0.251	0.049456	8.00	162	80607	OD initiation
	SN-6	0.2525	0.050049	6.26	125	2500000*	OD initiation
	SN-31	0.2515	0.049653	7.50	151	3500000*	OD initiation
SwRI HiPIPS Ti6Al4V	SN-4	0.251	0.049456	7.67	155	142028	OD initiation
	SN-17	0.2525	0.050049	7.76	155	1438410	OD initiation
	SN-5	0.2525	0.050049	7.76	155	95855	OD initiation
	SN-45	0.2525	0.050049	7.76	155	176966	OD initiation
	SN-36	0.251	0.049456	7.67	155	1540544	OD initiation
	SN-33	0.2525	0.050049	7.76	155	204887	OD initiation
CCAD	SN-13	0.258	0.052253	8.10	155	10129	OD initiation; multiple surface cracks noted
	SN-10	0.258	0.052253	8.10	155	10181	OD initiation; multiple surface cracks noted
	SN-30	0.2585	0.052455	8.14	155	9701	OD initiation; multiple surface cracks noted
	SN-29	0.263	0.054298	8.42	155	8082	OD initiation; multiple surface cracks noted
	SN-31	0.257	0.051848	8.04	155	11611	OD initiation; multiple surface cracks noted
SwRI HiPIPS CoCr	SN-9	0.253	0.050247	7.79	155	62948	OD initiation
	SN-46	0.252	0.049851	7.73	155	30315	OD initiation
	SN-40	0.2525	0.050049	7.76	155	39667	OD initiation
	SN-14	0.251	0.049456	7.67	155	38126	OD initiation
	SN-12	0.2515	0.049653	7.70	155	26146	OD initiation

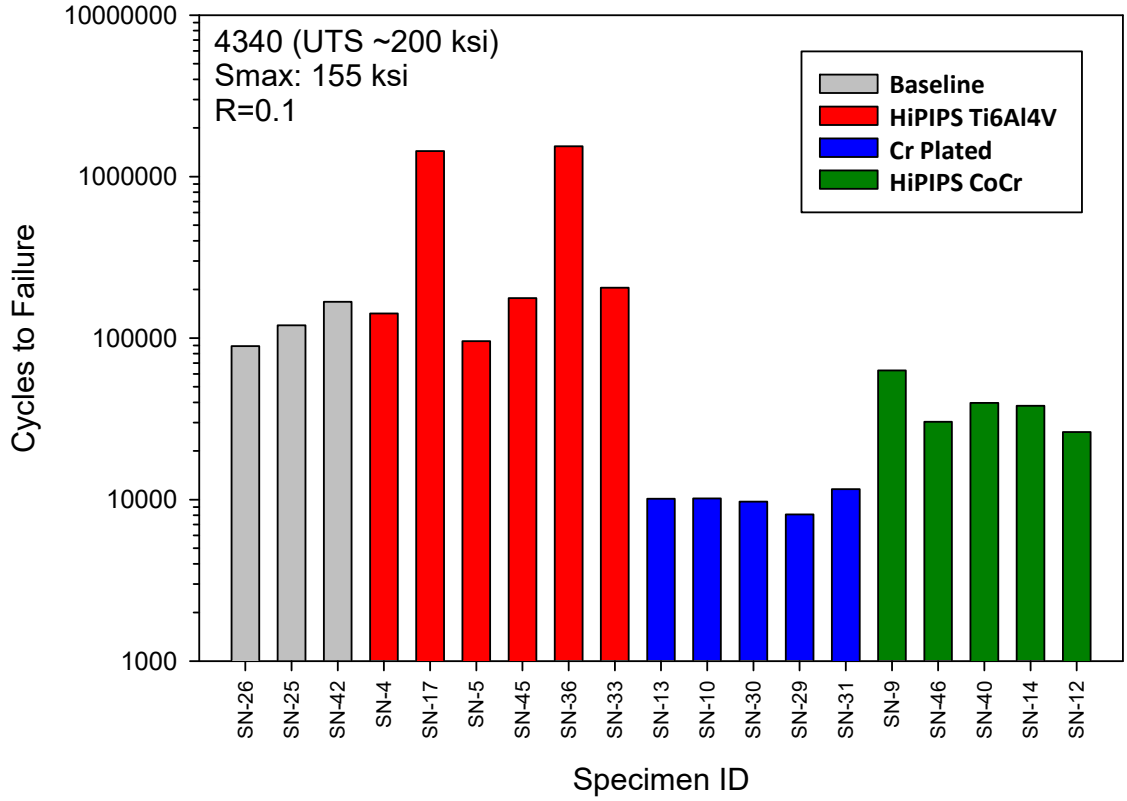

Figure 25. *Comparison of fatigue lives at 155 ksi for the four conditions evaluated (baseline and three surface treatments).*

5.0 Conclusions and Implications for Future Research

5.1 Conclusions

Altogether, the results of the project met the main objective to investigate the development of a new deposition technology that could reduce the costs and environmental risks in maintenance and replacement of military components. Specifically, the project investigated a novel atmospheric pressure, non-thermal HiPIPS for deposition of durable protective coatings and characterized the structural, mechanical and corrosion performance of the resultant coatings. The SwRI-developed HiPIPS is a promising candidate to revolutionize surface engineering and coating technologies. HiPIPS technology is unique in that this technology generates high density, high flux plasmas at low temperature and atmospheric pressure conditions. The HiPIPS technology provides an unparalleled plasma space that extends conventional atmospheric pressure plasma (APP) applications and allows for deposition of metallic coatings at ambient conditions. HiPIPS eliminates the need for vacuum chambers, high temperature processing and in-spray scenarios in surface treatments and deposition of coatings. The results of this project advanced the atmospheric pressure HiPIPS technique to TRL 4, validation in a laboratory environment to apply durable, metallic coatings.

At the end of the project, the following has been demonstrated through laboratory experiments.

- Designed and fabricated an advanced version of the atmospheric pressure HiPIPS jet head, which utilizes polymer casing along with a solid metal wire source material.
- Conducted HiPIPS investigations (over 50 experiments with Ar and Ti, CoCr, or Ti-6Al-4V wires) confirmed our hypothesis that high peak power pulses can be achieved (10-70 kW) resulting in high peak currents (100-250A) and increased ionization and plasma density while maintaining low overall power (40W) and substrate processing temperatures (< 50°C).
- Characterized the HiPIPS CoCr, Ti-6Al-4V and TiN plasma properties using current-voltage probes and OES.
- OES spectra confirmed the presence of Ti^{*} and Ti^{+*} with high phonon intensities in HiPIPS plasmas with Ar and Ti wire.
- OES spectra confirmed the presence of Ti^{*} and Ti^{+*}, along with Al^{*}, Al^{+*} and V^{*}, with high phonon intensities in HiPIPS plasma with Ar and Ti-6Al-4V wire.
- OES spectra confirmed the presence of Co^{*}, Cr^{*} and Cr^{+*} with high phonon intensities in HiPIPS plasmas with Ar and CoCr alloy wire.
- OES spectra of HiPIPS CoCr and Ar plasma showed no lines which could be assigned to higher (n>2) ionization states for Cr. Thus, the OES measurements verify the absence of any hex-Cr in HiPIPS CoCr plasma.
- OES spectra during the operation of HiPIPS with Ar and N_2 gases at a 1:1 ratio with a Ti electrode, did not detect characteristic Ar lines but detected lines attributed to Ti^{*} , Ti^{+*}, N_2 N_2^{+} species and atomic N.
- Conducted a systematic experimental study on the HiPIPS process parameters and resultant coating properties towards development of HiPIPS deposition of CoCr, Ti-6Al-4V and TiN coatings. Results indicate that a variation of process conditions can modify the deposit morphology from spherical nanoparticles towards that of a coating.
- Examined the microstructure and elemental composition of resulting deposited were examined using SEM and EDS.
- Cross-section SEM analysis revealed uniform coatings that ranged in thickness from 1 to 5 microns depending on deposition time.
- EDS mapping analysis revealed that the coating layer contains high amounts of chromium and cobalt for HiPIPS CoCr depositions.
- EDS mapping analysis revealed that the coating layer contained uniform and high amounts of Ti, Al and V for the HiPIPS Ti-6Al-4V depositions.
- EDS mapping analysis of coating from the operation of HiPIPS with Ar and N_2 (1:1) with a Ti electrode revealed that titanium and nitrogen are observed in the elemental composition of the resulting film.
- OES spectra successfully detected and identified charged state of the excited species in the plasma that corroborated the EDS analysis of the elemental composition in the resultant deposition coatings.
- Control samples were prepared using chrome plating services by the CCAD.
- Prepared HiPIPS Ti6Al4V and HiPIPS CoCr coatings on three (3) flat 4340 and aluminum alloy substrates for corrosion testing.
- Prepared HiPIPS SiOx bond layer coating only on aluminum alloy substrates for corrosion testing.
- Prepared HiPIPS Ti6Al4V and HiPIPS CoCr coatings on nine (9) 4340 dog-bone fatigue sample specimens.
- Performed XRD analysis on the as-deposited HiPIPS coating deposited using Ti electrode with Ar and N_2 gas at 1:1 ratio. The diffraction peaks related to different crystalline planes

of titanium nitride were observed.

- Conducted nano-hardness measurements on HiPIPS CoCr and HiPIPS Ti6Al4V coatings. The hardness of HiPIPS TiN, Ti6Al4V and CoCr films ranged from 11.56 to 14.09, 3.92 to 4.44, and 6.20 to 8.42 GPa, respectively.
- Completed GMW 14872 corrosion testing on SwRI-developed HiPIPS Ti6Al4V and CoCr coatings, conventional Cr plating techniques (CCAD plating), and uncoated samples for comparison. All coupons exhibited significant amounts of corrosion after 15 cycles of testing, including the conventionally Cr plated samples. The HiPIPS applied Ti6Al4V and CoCr coatings showed slightly more corrosion damage than the conventional coatings, but significantly less than that of the uncoated sample.
- Completed GMW 14872 testing on SwRI-developed HiPIPS CoCr coatings, SwRI HiPIPS SiOx bond layer coating, conventional Cr plating techniques (CCAD plating), and uncoated samples 7075 aluminum alloy samples for comparison. Aluminum coupons were tested for 42 cycles, longer than the 15 cycles for the steel coupons because the coatings on the aluminum coupons were less affected by the cyclic test. Samples coated with the HiPIPS CoCr coating and HiPIPS organosiloxane base layer alone (< 200 nm) coating performed better than the samples plated with the conventional coatings and the uncoated samples.
- Completed constant-amplitude load-controlled fatigue testing per ASTM E466 where baseline fatigue performance was compared to three surface treatments that included HiPIPS Ti6Al4V, HiPIPS CoCr and traditional Cr plating. When comparing the baseline response, the HiPIPS Ti6Al4V had a similar stress-life response and the HiPIPS CoCr was approximately half the fatigue life of the baseline conditions.

5.2 Implications for Future Research

Altogether, the project provided vital insight needed for the development of a new deposition technology that could reduce the costs and environmental risks in maintenance and replacement of military components. The results of this project advanced the atmospheric pressure HiPIPS technique to TRL 4, validation in a laboratory environment to apply durable, metallic coatings. The HiPIPS process is attractive for the repair or replacement of electroplated hard chromium in line-of-sight applications. HiPIPS is non-thermal, atmospheric pressure plasma capable of producing highly ionized species for deposition of durable films. Processing temperatures are ≤ 150 °C. HiPIPS operates solely with an inert carrier gas (i.e., Ar, N_2) and solid metallic wire/rod source material. While this project focused on demonstration of CoCr, Ti6Al4V, and TiN films, the HiPIPS process is widely applicable to other coating chemistries. Additionally, HiPIPS could allow for coating removal, pre-cleaning, and coating using the same equipment and varying process parameters. Substrates require no special surface preparation, substrate heating, or extensive post-treatments. HiPIPS has a fine level of control over deposition thickness, reducing post application machining. A HiPIPS system is portable and can be operated in versatile environments. Further development work is required to increase the technology readiness level and identify specific applications. More specifically, additional development work is needed to i) scale-up the HiPIPS source in order to allow for increased build rate as well as larger area coverage, and ii) to progress the demonstrated laboratory prototype system into a packaged, deployable unit with robotic automation. Logical next research steps include experiments in returning damaged components to dimensional tolerance with benchmark surface finish and mechanical properties. Research focused on substrate interfaces and how initial coating layers or pretreatments can influence coating adhesion and corrosion resistance would be advantageous.

6.0 Literature Cited

1. Khaled, T. "A Look at Hard Chrome Replacement" Federal Aviation Administration Report # ANM-112-01-01 Rev A January 2002.

2. Legg, K; Sauer, J. "Use of Thermal Spray as an Aerospace Chrome Plating Alternative" Final Report for Joint Strike Fighter Program Office. Contract N00173-98-D-2000 DO 0002. October 27, 2000.

3. Navinsˇek, B.; Panjan, P.; Milosˇev, I. "PVD Coatings as an Alternative to Electroplating and Electroless Processes" Surface Coatings Technology. 1999. 116, 476-486.

4. Pfender, E. "Fundamental Studies Associated with the Plasma Spray Process" Surface Coatings Technology. 1988. 34, 1-14.

5. Poenitzsch, V.Z.; Wei, R.; Coulter, K. E. "Low-Temperature, High Flux Process Space for High Power Impulse Plasma Source" DARPA Contract # HR0011-13-C-0008 (2013)

6. Poenitzsch, V.Z.; Wei, R.; Coulter, K. E., Langa, E. "*High Power Impulse Plasma Source*" Invention Disclosure Docket No. 3706, August 12, 2013.

7. Poenitzsch, V.Z.; Wei, R.; Coulter, K. E., Langa, E. "*Apparatus of Atmospheric Pressure Pulsed Arc Plasma Source and Method for Depositing of Coatings*" Invention Disclosure Docket No. 3797, February 26, 2015.

8. Kramida, A., Ralchenko, Yu, Reader, J. and NIST ASD Team (2017). *NIST Atomic Spectra Database* (version 5.5.1), [Online]. Available: https://physics.nist.gov/asd [Thu Nov 09 2017]. National Institute of Standards and Technology, Gaithersburg, MD.

9. Timmermans, E. A. H.; Jonkers, J.; Thomas, I. A. J.; Rodero, M. C.; Quintero, A.; Sola, A. Gamero, A.; van der Mullen, J. A. A. "The Behavior of Molecules in Microwave-induced Plasmas Studied by Optical Emission Spectroscopy" Spectrochimica Act Part B: Atomic Spectroscopy. 1998. 53, 1553-1556.

Appendix A: List of Scientific/Technical Publications

The following scientific/technical publications were produced during the course of the project:

1. Articles in Peer-Reviewed Journals:

    a. Poenitzsch, V., Wei, R., Miller, M. A., Coulter, K. (2019) Atmospheric Pressure High Power Impulse Plasma Source for Deposition of Metallic Coatings. *Journal of Materials Research*, 34(12), 2078-2085. doi:10.1557/jmr.2019.184

2. Conference or Symposium Abstracts:

    a. Poenitzsch, V.Z., Macha, E., Wei, R., Martinez, R. "Novel Atmospheric High Power Impulse Plasma Source for Durable, Field Applicable Coatings" ASETS Defense Workshop, Orlando, FL, December 2016.

    b. Poenitzsch, V.Z., Macha, E., Wei, R. "Novel Atmospheric High Power Impulse Plasma Source for Durable, Field Applicable Coatings" 2017 SERDP and ESTCP Symposium, November 2017.

    c. Poenitzsch, V.Z., Macha, E., Wei, R. "Novel Atmospheric High Power Impulse Plasma Source for Durable, Field Applicable Coatings" 2017 SERDP and ESTCP Symposium, November 2018.

    d. Poenitzsch, V.Z., Macha, E., Wei, R. "Atmospheric Pressure High Power Impulse Plasma Source for Deposition of Metallic Coatings" 2018 Materials Research Society (MRS) Conference, November 2018.

Appendix B: Other Supporting Materials

The following patents and technical awards were completed during the course of the project:

1. Patents:

    a. V.Z. Poenitzsch, R. Wei, E. Langa, K.E. Coulter "Atmospheric Pressure Pulsed Arc Plasma Source and Methods of Coating Wherein" U.S. Patent 10,354,845 B2.

2. Awards:

    a. "High Power Impulse Plasma Source (HiPIPS)" 2017 R&D 100 Award Winner.